Title

Adaptive Robust Formation Control of Connected and Autonomous Vehicle Swarm System Based on Constraint Following

Journal

IEEE Transactions on Cybernetics, 53(7)

ISSN

2168-2267

Authors

Sun, Qinqin
Wang, Xiuye
Yang, Guolai
et al.

Publication Date

2023-07-01

DOI

10.1109/tcyb.2022.3150032

Peer reviewed

Adaptive Robust Formation Control of Connected and Autonomous Vehicle Swarm System Based on Constraint Following

Qinqin Sun, Xiuye Wang, Guolai Yang, Ye-Hwa Chen, and Fai Ma

***Abstract*—This article proposes an adaptive robust formation control scheme for the connected and autonomous vehicle (CAV) swarm system by utilizing swarm property, diffeomorphism transformation, and constraint following. The control design is processed by starting from a 2-D dynamics model with (possibly fast) time varying but bounded uncertainty. The uncertainty bounds are unknown. For compact formation, the CAV system is treated as an artificial swarm system, for which the ideal swarm performance is taken as a desired constraint. By this, formation control is converted into a problem of constraint following and then a performance measure β is defined as the control object to evaluate the constraint following error. For collision avoidance, a diffeomorphism transformation on space measure between two vehicles is creatively performed, by which the space measure is positive restricted. For uncertainty handling, an adaptive robust control scheme is proposed to render the β-measure to be uniformly bounded and uniformly ultimately bounded, that is, drive the controlled (CAV) swarm system to follow the desired constraint approximatively. As a result, the system can achieve the ideal swarm performance; thereout, compact formation is realized, regardless of the uncertainty. The main contribution of this article is exploring a 2-D formation control scheme for (CAV) swarm system under the consideration of collision avoidance and time-varying uncertainty.**

***Index Terms*—Adaptive robust control, constraint following, diffeomorphism transformation, formation control, swarm system.**

Manuscript received 18 January 2021; revised 6 August 2021; accepted 5 February 2022. Date of publication 23 February 2022; date of current version 16 June 2023. This work was supported in part by the National Natural Science Foundation of China under Grant 52175099; in part by the China Postdoctoral Science Foundation under Grant 2020M671494; in part by the Jiangsu Planned Projects for Postdoctoral Research Funds under Grant 2020Z179; in part by the Nanjing University of Science and Technology Independent Research Program under Grant 30920021105; and in part by the Fundamental Research Funds for the Central Universities under Grant 300102259306. This article was recommended by Associate Editor T. H. Lee. *(Corresponding author: Xiuye Wang.)*

Qinqin Sun is with the School of Energy and Power Engineering, Nanjing University of Aeronautics and Astronautics, Nanjing 210016, Jiangsu, China (e-mail: sun421529@126.com).

Xiuye Wang and Guolai Yang are with the School of Mechanical Engineering, Nanjing University of Science and Technology, Nanjing 210094, Jiangsu, China (e-mail: xiuyewang@126.com; yyanggl@njust.edu.cn).

Ye-Hwa Chen is with the George W. Woodruff School of Mechanical Engineering, Georgia Institute of Technology, Atlanta, GA 30332 USA, and also with the Key Laboratory of Road Construction Technology and Equipment of MOE, Chang'an University, Xi'an 710064, Shanxi, China (e-mail: yehwa.chen@me.gatech.edu).

Fai Ma is with the Department of Mechanical Engineering, University of California at Berkeley, Berkeley, CA 94720 USA (e-mail: fma@berkeley.edu).

Color versions of one or more figures in this article are available at https://doi.org/10.1109/TCYB.2022.3150032.

Digital Object Identifier 10.1109/TCYB.2022.3150032

I. Introduction

As a typical connected and autonomous vehicle (CAV) system, autonomous vehicle platoon system has attracted many researchers' attentions in the past two decades [1]–[6]. Their primary focus is on *road vehicles* and the associated issues, such as traffic congestion, fuel consumption, driving safety, etc., in which the (road) vehicle is supposed to drive in a marked lane on the road and the motion is usually simplified to be longitudinal *linear*. However, with the development of technology, a variety of autonomous *functional vehicles* has appeared, such as unmanned road roller (in engineering), unmanned ground vehicle (in military), automatic guided vehicle (in industry), etc. As IoT techniques seep in, such functional vehicles also can be connected as an autonomous vehicle platoon for collaborative tasks. In this sense, the agent of the autonomous vehicle platoon system is no longer confined to road vehicles; meanwhile, the trajectory is no longer a marked lane on the road but may be an arbitrary curve determined by the work scenario. By this, the previous studies [1]–[6] that mainly focus on *linear* motion of the autonomous vehicle platoon system are inadequate, and more explorations on *planar* motion, including longitudinal motion and lateral motion, are expected. Motivated by this, this article focuses on a *2-D* platooning problem (i.e., formation control) of CAV systems. This is the first set of contribution and innovation of this article.

In formation control of CAV systems, two objectives should be achieved: 1) *compact formation* and 2) *collision avoidance* [3]. The first is for consistency and synergy of the vehicles when they carry out a collaborative task. The second is for safety. Many works have been done for the first objective of compact formation in the past. As an outstanding representative in this field, Chen *et al.* ([3]–[7] and their bibliographies) have addressed this from a novel perspective of artificial swarm system. They took the CAV system as an artificial swarm system, and then designed an appropriate control to drive it to render ideal swarm performance, by which the distance between two vehicles was neither too far nor too close, such that compact formation was achieved. They did

the first work that addresses artificial swarm system issues in both kinematic and dynamic phases, while the existing related works usually (only) involve to kinematic phase. Along Chen's methodology [3]–[7], this article handles the CAV system as an artificial swarm system and explores its planar motion in both kinematic and dynamic phases. This is the second set of contribution and innovation of this article. For this, we call the CAV system with N agents as a CAV *swarm* system in this article.

The second objective of collision avoidance is a very common issue in practical engineering (not limited to CAV system), for which many works have been done from the perspectives of application and experiment [8], [9], however, for methodological study, few outstanding work have been done. As representative research, Aggarwal and Leitmann [10], Leitmann and Skowronski [11], Corless *et al.* [12], and Corless and Leitmann [13] explored a pioneering approach of collision avoidance control starting from the definition of uniform boundedness; Petrosjan [14] solved the problem of pursuit-evasion with an application of noncooperative zero-sum game theoretic; Stipanovic *et al.* [15] proposed a cooperative control of collision avoidance for multiagent systems. In recent years, Chen *et al.* ([2]–[7], [16], [17], and their bibliographies) have opened up a new way of collision avoidance control based on diffeomorphism transformation. By introducing state transformation into control design, their proposed control can drive the system to render two layers performance: 1) collision avoidance and 2) stability (i.e., uniform boundedness and uniform ultimate boundedness), regardless of the system uncertainty. Along this way [2]–[7], [16], and [17], this article excepts to address three problems in the CAV swarm system simultaneously: 1) *collision avoidance*; 2) *uncertainty handling*; and 3) *formation control*. This is the third set of contribution and innovation of this article.

System uncertainty is inevitable in the CAV swarm system and has a significant impact on system performance; hence, uncertainty handling is very important in precise formation control. In the past, many efforts on uncertainty handling have been done [18]–[25]. Wang *et al.* [26] proposed an adaptive finite-time fault-tolerant control scheme for the nonlower-triangular nonlinear systems. This article brings to an alternative method. The uncertainty considered in this article is (possibly fast) time varying but bounded, and the bounds are unknown but their comprehensive effect on system performance can be estimated with an adaptive parameter online. By taking the ideal swarm performance of the concerned CAV swarm system as a servo constraint, formation control is formulated as a task of constraint following, that is, design proper control to drive the system to follow the constraint approximatively. For this, two partial controllers are proposed: one aims at driving the *nominal* system to follow the constraint strictly and the other one aims at driving the *uncertain* portions of the system to follow the constraint approximatively. Under the combined action of these two, the entire system can render approximate constraint following [27].

This article possesses four significant *contributions*. First, it extends formation control of CAV swarm system from a traditional *linear* issue to a more generalized *planar* issue. By this, both longitudinal motion and lateral motion are involved, based on which a 2-D formation control problem is explored. Second, for compact formation, a constraint-following framework is constructed by taking the ideal swarm performance of the concerned CAV swarm system as a desired constraint. Third, for collision avoidance, a diffeomorphism transformation on space measure between two vehicles is creatively performed, by which the space measure is positive restricted, while the transformed variable (i.e., the swarm variable) is unrestricted, such that control design can be out of state restriction. Forth, for uncertainty handling, an adaptive robust control scheme is proposed to drive the concerned CAV swarm system to follow the desired constraint approximately, that is, render the ideal swarm performance, even with time-varying uncertainty.

II. Preliminaries: Artificial Swarm System

Consider an artificial swarm system with N agents. The *ideal kinematic performance* of each agent $i \in \mathcal{N}, \mathcal{N} = \{1, 2, \ldots, N\}$, is described by

$$\dot{q}_i = -\sum_{j=1, j\neq i}^{N} \frac{\partial G_{ij}}{\partial q_i}(q_i, q_j). \tag{1}$$

Here, $q_i \in \mathbf{R}^n$ is the state vector, and $G_{ij}(\cdot) : \mathbf{R}^n \times \mathbf{R}^n \to \mathbf{R}$ is smooth and shows the influence of agent j on i. By (1), we can see that the accumulation of all influence by other agents then affects i. Combination of the *ideal kinematic performance* of each agent as (1) is called as *ideal swarm performance* thereafter.

Define $g_{ij}(q_i, q_j) \coloneqq \partial G_{ij}/\partial q_i(q_i, q_j)$ and then we have the following properties [28], [29].

Property 1 (State Dilation): For each $i, j \in \mathcal{N}$, there is a mapping $\hat{G}_{ij}(\cdot) : \mathbf{R}^n \to \mathbf{R}$ such that

$$G_{ij}(q_i, q_j) = \hat{G}_{ij}(q_i - q_j). \tag{2}$$

Property 2 (Symmetry): For each $i, j \in \mathcal{N}$

$$G_{ij}(q_i, q_j) = G_{ji}(q_j, q_i). \tag{3}$$

Property 3 (Monoticity in Repulsion/Attraction): For each $i, j \in \mathcal{N}$, there exists a ball $\mathcal{B}_{\delta_{ij}}(q_i)$, with radius δ_{ij} and center q_i, such that: 1) if $q_j \in \text{ int } \mathcal{B}_{\delta_{ij}}(q_i)$, then $(q_i - q_j)^T g_{ij} < 0$ and 2) if $q_j \notin \mathcal{B}_{\delta_j}(q_i)$, then $(q_i - q_j)^T g_{ij} > 0$.

Property 4 (Linear Factorization): There is a function $\bar{g}_{ij}(q_i, q_j)$, by which the function $g_{ij}(\cdot)$ can be linearly factorized with respect to $q_i - q_j$ as follows:

$$g_{ij}(q_i, q_j) = (q_i - q_j)\bar{g}_{ij}(q_i, q_j). \tag{4}$$

Furthermore, there are scalar constants $a > 0, \phi_{ij} > 0$ such that

$$\left\| (q_i - q_j)\left(\bar{g}_{ij}(q_i, q_j) - a\right) \right\| \leq \phi_{ij} \tag{5}$$

for all q_i and q_j.

Remark 1: Property 1 means the influence of agent j on i is uniquely determined by the relative position between agent i and j. Property 2 means the roles acted by q_i on q_j and q_j on

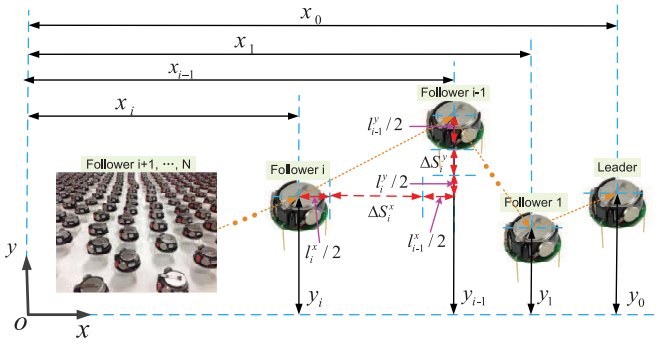

Fig. 1. CAV swarm system.

q_i are the same. Property 3 means the repulsion or attraction action between agents i and j (i.e., the direction of g_{ij}) is uniquely determined by the relative position $q_i - q_j$; thus, the relative distance between agent i and j will not be too close or too far away. This is the key factor for an ideal artificial swarm system to have the capability of automatic formation. Property 4 means the function $g_{ij}(\cdot)$ can be linearly factorized with respect to $q_i - q_j$.

The above analysis shows that subject to the ideal swarm performance, an artificial swarm system can render the aforementioned Properties 1–4. In this sense, by taking the system dynamic into account, if we can design an appropriate control to drive all the agents to subject to the ideal kinematic performance as (1), the system will render the aforementioned properties; hence, the desired dynamic behavior of automatic formation is achieved. Inspired by this, this article treats the CAV system as an artificial swarm system and proposes an adaptive control to drive it to subject to the ideal swarm performance for automatic formation. For control design, the ideal swarm performance is addressed as a servo constraint, based on which a problem of approximate constraint-following control is carried out later on (see Section V).

III. Dynamic Model of Connected Autonomous Vehicle Swarm Systems

Consider a connected autonomous vehicle (CAV) swarm system consisting of $N+1$ vehicles driving on 2-D ground. Shown as Fig. 1, $x-o-y$ is the ground-fixed coordinate frame with origin o, l_0^x and l_i^x, respectively, show the lengths of the leader (i.e., the vehicle 0) and the follower i (i.e., the vehicle i), l_0^y and l_i^y, respectively, show the widths of the leader and the follower i, $x_0 \in \mathbf{R}$ and $y_0 \in \mathbf{R}$, respectively, denote the positions in x and y directions of the leader, meanwhile, $x_i \in \mathbf{R}$ and $y_i \in \mathbf{R}$, respectively, denote the positions in x and y directions of the follower i. We would like to emphasize that the formation shown as Fig. 1 is only a schematic, while in practice, it may be different in different cases (such as a one-line type, a triangular type, a trapezoidal type, etc.).

Let $X_0 := [x_0\ y_0]^T$ and $X_i := [x_i\ y_i]^T$. They, respectively, denote the positions of the leader and the follower i; thereout, $\dot{X}_0 = [\dot{x}_0\ \dot{y}_0]^T$, $\ddot{X}_0 = [\ddot{x}_0\ \ddot{y}_0]^T$, $\dot{X}_i = [\dot{x}_i\ \dot{y}_i]^T$, and $\ddot{X}_i = [\ddot{x}_i\ \ddot{y}_i]^T$. Let $\tau_0 := [\tau_0^x\ \tau_0^y]^T$ and $\tau_i := [\tau_i^x\ \tau_i^y]^T$. They, respectively, denote the control input of the leader and the follower i. The leader can be seen as a *virtual* vehicle for the purpose of positioning and guiding. The motion equation of it is described as

$$M_0\ddot{X}_0(t) = \tau_0(t) \tag{6}$$

where $\ddot{X}_0 \in \mathbf{R}^2$ is the acceleration, $t \in \mathbf{R}$ is the time, and $M_0 \in \mathbf{R}^2$, $M_0 > 0$ is the inertia matrix. The motion equation of follower i is described as

$$\begin{aligned} &M_i(X_i(t), \sigma_i(t), t)\ddot{X}_i(t) + C_i\big(X_i(t), \dot{X}_i(t), \sigma_i(t), t\big) \\ &\quad + F_i\big(X_i(t), \dot{X}_i(t), \sigma_i(t), t\big) = \tau_i(t) \end{aligned} \tag{7}$$

where $\dot{X}_i \in \mathbf{R}^2$ is the velocity, $\ddot{X}_i \in \mathbf{R}^2$ is the acceleration, $\sigma_i \in \Sigma_i \subset \mathbf{R}^{p_i}$ is the uncertain parameter, which is (possibly fast) time varying but bounded, and $\Sigma_i \subset \mathbf{R}^{p_i}$ is compact and denotes the possible bounding of σ_i. What is more, $M_i \in \mathbf{R}^2$, $M_i > 0$ is the inertia matrix, $C_i(X_i, \dot{X}_i, \sigma_i, t) \in \mathbf{R}^2$ is the aerodynamic drag force, and $F_i(X_i, \dot{X}_i, \sigma_i, t) \in \mathbf{R}^2$ is the collection rolling resistance force, acceleration resistance, and other external disturbances. The functions $M_i(\cdot)$, $C_i(\cdot)$, and $F_i(\cdot)$ are all continuous.

For later formation control, we define an *actual horizontal space* between vehicle i and its preceding vehicle $i-1$ as

$$\Delta S_i^x(t) = |x_{i-1}(t) - x_i(t)| - \frac{l_{i-1}^x + l_i^x}{2} \tag{8}$$

and an *actual vertical space* as

$$\Delta S_i^y(t) = |y_{i-1}(t) - y_i(t)| - \frac{l_{i-1}^y + l_i^y}{2}. \tag{9}$$

As the vehicle i may be in front or behind (up or down) of the vehicle $i-1$, it is not sure which is larger, x_{i-1} or x_i (y_{i-1} or y_i); hence, the signs of $x_{i-1} - x_i$ and $y_{i-1} - y_i$ are not sure. For this, we number the vehicles naturally, that is, suppose vehicle i is after vehicle $i-1$; hence, $x_{i-1} - x_i > 0$.

For the sake of analysis, we introduce a *horizontal space measure* as

$$\widetilde{S}_i^x(t) = x_{i-1}(t) - x_i(t) - \frac{l_{i-1}^x + l_i^x}{2} \tag{10}$$

to measure the actual horizontal space ΔS_i^x and a *vertical space measure* as

$$\widetilde{S}_i^y(t) = (y_{i-1}(t) - y_i(t))^2 - \left(\frac{l_{i-1}^y + l_i^y}{2}\right)^2 \tag{11}$$

to measure the actual vertical space ΔS_i^y. Shown as Fig. 1, the actual horizontal space ΔS_i^x (8) and the actual vertical space ΔS_i^y (9) are greater than zero, meanwhile, their alternatives $\widetilde{S}_i^x$ (10) and $\widetilde{S}_i^y$ (11)) are also greater than zero.

As the signs of $\widetilde{S}_i^x$, $\widetilde{S}_i^y$, and ΔS_i^x, ΔS_i^y are coincident, we use $\widetilde{S}_i^x$, $\widetilde{S}_i^y$ as in (10)-(11) to replace ΔS_i^x, ΔS_i^y as in (8) and (9) as an *indirect* measurement of space between two adjacent vehicles in the following analysis. Suppose the vehicle i and its preceding vehicle $i-1$ except to keep at a *desired horizontal space* $\bar{S}_i^x$ and a *desired vertical space* $\bar{S}_i^y$. $\bar{S}_i^x$ and $\bar{S}_i^y$ are positive constant scalars. Let $S_i^x := \bar{S}_i^x$ and $S_i^y := (\bar{S}_i^y)^2$. We then define a *horizontal space error* as

$$e_i^x(t) := S_i^x - \widetilde{S}_i^x(t) \tag{12}$$

and a *vertical space error* as

$$e_i^y(t) := S_i^y - \widetilde{S}_i^y(t). \tag{13}$$

With (10) and (11), we have

$$\begin{aligned} e_i^x(t) &= S_i^x - x_{i-1}(t) + x_i(t) + \frac{l_{i-1}^x + l_i^x}{2} \\ e_i^y(t) &= S_i^y - (y_{i-1}(t) - y_i(t))^2 + \left(\frac{l_{i-1}^y + l_i^y}{2}\right)^2. \end{aligned} \tag{14}$$

It is practical and important for the CAV swarm system to avoidance collision in the process of formation marching. For this, besides of formation control, collision avoidance is especially addressed in this article. This brings to the following definition.

Definition 1: For any initial safe condition (i.e., $\widetilde{S}_i^x(t_0) > 0$) and $\widetilde{S}_i^y(t_0) > 0$), the CAV swarm system demonstrates *collision avoidance* if $\widetilde{S}_i^x(t) > 0$ and $\widetilde{S}_i^y(t) > 0$ [i.e., $e_i^x(t) < S_i^x$ and $e_i^y(t) < S_i^y$] for all $t > t_0$.

Remark 2: $\widetilde{S}_i^x > 0$ and $\widetilde{S}_i^y > 0$ can be seen as the original state of the CAV swarm system. In practical, if the space measures $\widetilde{S}_i^x$ and $\widetilde{S}_i^y$ are less than or equal to zero in a same time, the vehicles will hit each other; hence, $\widetilde{S}_i^x > 0$ and $\widetilde{S}_i^y > 0$ are excepted for collision avoidance. On the contrary, if any one of them is too large, the related vehicle will fall behind; hence, relatively small $\widetilde{S}_i^x$ and $\widetilde{S}_i^y$ are excepted for compact formation. This article aims at an equilibrium solution for such two seemingly conflicting issues of *collision avoidance* and *compact formation*. This is one of the salient features of this article.

IV. State Transformation for Collision Avoidance

Recalling the definition of collision avoidance as Definition 1, it imposes positive restrictions on $\widetilde{S}_i^x$ and $\widetilde{S}_i^y$ (i.e., $\widetilde{S}_i^x > 0$ and $\widetilde{S}_i^y > 0$), for which a standard control method that designs control directly for $\widetilde{S}_i^x$ and $\widetilde{S}_i^y$ would be invalid. For this, this article proposes an indirect control approach by transforming $\widetilde{S}_i^x$ and $\widetilde{S}_i^y$ into other variables $q_i^x \in \mathbf{R}$ and $q_i^y \in \mathbf{R}$. The transformation is described as

$$\widetilde{S}_i^x = S_i^x \exp(q_i^x), \quad \widetilde{S}_i^y = S_i^y \exp(q_i^y). \tag{15}$$

Remark 3: It is easy to see that as $\exp(q_i^x), \exp(q_i^y) > 0$ and $S_i^x, S_i^y > 0$, the transformation will result in strictly positive $\widetilde{S}_i^x, \widetilde{S}_i^y$ for any $|q_i^x|, |q_i^y| < \infty$; thus, collision avoidance is assured. Furthermore, $\widetilde{S}_i^x$ and $\widetilde{S}_i^y$ are assured to be bounded with bounded q_i^x and q_i^y.

As this transformation is bijective, we, in turn, have

$$q_i^x = \ln\left(\frac{\widetilde{S}_i^x}{S_i^x}\right), \quad q_i^y = \ln\left(\frac{\widetilde{S}_i^y}{S_i^y}\right). \tag{16}$$

Note that $\widetilde{S}_i^x$ as in (10) denotes a measure of the horizontal space between two adjacent vehicles, while $\widetilde{S}_i^y$ as in (11) denotes a measure of the vertical space. If the values of $\widetilde{S}_i^x$ and $\widetilde{S}_i^y$ are greater than zero, the two adjacent vehicles will not collide. In other words, as long as the two adjacent vehicles do not collide, the values of $\widetilde{S}_i^x$ and $\widetilde{S}_i^y$ are always greater than zero. As the later proposed controller has the ability of anti-collision, as long as the initial states of the vehicles are reasonable (i.e., ensured not to collide), they will never collide. By this, as long as the initial values of $\widetilde{S}_i^x$ and $\widetilde{S}_i^y$ are greater than zero, they will always be greater than zero. Therefore, the natural log function here will always be greater than zero.

Using (10) and (11) in (16), we then have

$$\begin{aligned} x_i &= x_{i-1} - S_i^x \exp(q_i^x) - \frac{l_{i-1}^x + l_i^x}{2} \\ y_i &= y_{i-1} - \left(S_i^y \exp(q_i^y) + \frac{(l_{i-1}^y + l_i^y)^2}{4}\right)^{\frac{1}{2}}. \end{aligned} \tag{17}$$

Let $L_i^x := (l_{i-1}^x + l_i^x)/2$ and $L_i^y := (l_{i-1}^y + l_i^y)^2/4$. L_i^x and L_i^y are positive constant scalars. Taking the second-order derivative of x_i and y_i with respect to t, we have

$$\begin{aligned} \ddot{x}_i &= \ddot{x}_{i-1} - S_i^x \exp(q_i^x)(\dot{q}_i^x)^2 - S_i^x \exp(q_i^x)\ddot{q}_i^x, \\ \ddot{y}_i &= \ddot{y}_{i-1} - \frac{1}{2}S_i^y \exp(q_i^y)(S_i^y \exp(q_i^y) + L_i^y)^{-\frac{1}{2}}(\dot{q}_i^y)^2 \\ &\quad + \frac{1}{4}(S_i^y \exp(q_i^y))^2(S_i^y \exp(q_i^y) + L_i^y)^{-\frac{3}{2}}(\dot{q}_i^y)^2 \\ &\quad - \frac{1}{2}S_i^y \exp(q_i^y)(S_i^y \exp(q_i^y) + L_i^y)^{-\frac{1}{2}}\ddot{q}_i^y. \end{aligned} \tag{18}$$

Denote

$$\begin{aligned} H_i^x(q_i^x, \dot{q}_i^x) &:= -S_i^x \exp(q_i^x)(\dot{q}_i^x)^2 \\ H_i^y(q_i^y, \dot{q}_i^y) &:= -\frac{1}{2}S_i^y \exp(q_i^y)(S_i^y \exp(q_i^y) + L_i^y)^{-\frac{1}{2}}(\dot{q}_i^y)^2 \\ &\quad + \frac{1}{4}(S_i^y \exp(q_i^y))^2(S_i^y \exp(q_i^y) + L_i^y)^{-\frac{3}{2}}(\dot{q}_i^y)^2 \\ Q_i^x(q_i^x) &:= -S_i^x \exp(q_i^x) \\ Q_i^y(q_i^y) &:= -\frac{1}{2}S_i^y \exp(q_i^y)(S_i^y \exp(q_i^y) + L_i^y)^{-\frac{1}{2}}. \end{aligned} \tag{19}$$

Taking them into (18), we have

$$\begin{aligned} \ddot{x}_i &= \ddot{x}_{i-1} + H_i^x + Q_i^x \ddot{q}_i^x \\ \ddot{y}_i &= \ddot{y}_{i-1} + H_i^y + Q_i^y \ddot{q}_i^y. \end{aligned} \tag{20}$$

Let $q_i := [q_i^x \ q_i^y]^T$, $q_i \in \mathbf{R}^2$; thereout, $\dot{q}_i = [\dot{q}_i^x \ \dot{q}_i^y]^T$ and $\ddot{q}_i = [\ddot{q}_i^x \ \ddot{q}_i^y]^T$, with which we define

$$\begin{aligned} H_i(q_i, \dot{q}_i) &:= \begin{bmatrix} H_i^x(q_i^x, \dot{q}_i^x) \\ H_i^y(q_i^y, \dot{q}_i^y) \end{bmatrix} \\ Q_i(q_i) &:= \begin{bmatrix} Q_i^x(q_i^x) & 0 \\ 0 & Q_i^y(q_i^y) \end{bmatrix}. \end{aligned} \tag{21}$$

With it, we can rewrite (20) in matrix form as

$$\ddot{X}_i = \ddot{X}_{i-1} + H_i + Q_i \ddot{q}_i. \tag{22}$$

With (7), we have

$$\ddot{X}_i = M_{i-1}^{-1}(\tau_{i-1} - C_{i-1} - F_{i-1}) + H_i + Q_i \ddot{q}_i. \tag{23}$$

Substituting it into (7), the CAV swarm system as (7) is redescribed as

$$\begin{aligned} &M_i Q_i \ddot{q}_i + C_i + F_i + M_i H_i \\ &\quad + M_i M_{i-1}^{-1}(\tau_{i-1} - C_{i-1} - F_{i-1}) = \tau_i. \end{aligned} \tag{24}$$

We then would like to incorporate the swarm performance into the transformed state q_i. Suppose it is constrained by the

ideal kinematic performance as (1). Let $\bar{q}^x := (1/N)\sum_{i=1}^N q_i^x$ and $\bar{q}^y := (1/N)\sum_{i=1}^N q_i^y$, and define $\bar{q} := [\bar{q}^x\ \bar{q}^y]^T$ as the *swarm center*. Let $\widetilde{S}^x := \prod_{i=1}^N \widetilde{S}_i^x$ and $\widetilde{S}^y := \prod_{i=1}^N \widetilde{S}_i^y$, and define $\widetilde{S} := [\widetilde{S}^x\ \widetilde{S}^y]^T$ as the collection of actual space. Let $S^x := \prod_{i=1}^N S_i^x$ and $S^y := \prod_{i=1}^N S_i^y$, and define $S := [S^x\ S^y]^T$ as the collection of ideal space. We then reach to the following performance.

Theorem 1: The product of $\widetilde{S}_i^x$ and $\widetilde{S}_i^y$ remains unchanged for all time: $\widetilde{S} = [S^x \exp(N\bar{q}^x(t_0))\ S^y \exp(N\bar{q}^y(t_0))]^T$.

Proof: According to [28], we have

$$\begin{aligned}\bar{q}^x(t) &= \bar{q}^x(t_0), t \geq t_0\\ \bar{q}^y(t) &= \bar{q}^y(t_0), t \geq t_0.\end{aligned} \tag{25}$$

Recalling $q_i^x = \ln(\widetilde{S}_i^x/S_i^x)$ as (16), we have

$$\sum_{i=1}^N \ln\left(\frac{\widetilde{S}_i^x}{S_i^x}\right) = \sum_{i=1}^N q_i^x = N\bar{q}^x(t) = N\bar{q}^x(t_0) \tag{26}$$

such that

$$\ln\left(\prod_{i=1}^N \frac{\widetilde{S}_i^x}{S_i^x}\right) = N\bar{q}^x(t_0). \tag{27}$$

We then have

$$\prod_{i=1}^N \widetilde{S}_i^x = \prod_{i=1}^N S_i^x \exp\left(N\bar{q}^x(t_0)\right) \tag{28}$$

that is

$$\widetilde{S}^x = S^x \exp\left(N\bar{q}^x(t_0)\right). \tag{29}$$

Similarly, we have

$$\widetilde{S}^y = S^y \exp\left(N\bar{q}^y(t_0)\right). \tag{30}$$

With $\widetilde{S} = [\widetilde{S}^x\ \widetilde{S}^y]^T$, we have

$$\widetilde{S} = \left[S^x \exp\left(N\bar{q}^x(t_0)\right)\ S^y \exp\left(N\bar{q}^y(t_0)\right)\right]^T. \tag{31}$$

■

Remark 4: With Theorem 1, we can see that the state transformation as (15) not only implies the collision avoidance condition $\widetilde{S}_i^x(t), \widetilde{S}_i^y(t) > 0$ but also renders to global performance.

Remark 5: Recalling the concept of *constraint following*, it means to drive the system to follow a constraint. In mechanical systems, the prescribed (desired) system performance can be always represented as constraint. If we want to drive the mechanical system to perform in a certain way, we can design a control to drive the system to follow the desired constraint. This is the so-called constraint following control. As for the formation control of the CAV swarm system, if we can design an appropriate control to drive the transformed state q_i to (approximatively) subject to the constraint as (1), the controlled CAV swarm system not only renders the swarm Properties 1–4 but also possesses the global invariance described as Theorem 1. By this, a problem of approximatively constraint following control is arisen.

Remark 6: The constraint following refers to (servo) constraint about the state (i.e., the coordinate), velocity, acceleration, or even a combination of them, while the state constraints (shown as in [30]) refers to constraint only about the state. By this, no limitation on practical implication of constraint exists in the constraint following. In this sense, compared with the control for state constraints, control for constraint following can solve a wider range of control problems and achieve more complex control goals. This reflects the advantages of constraint-following control.

V. Adaptive Robust Control for Approximate Constraint Following

By taking the ideal kinematic performance (1) as desired constraint on the CAV swarm system, an adaptive robust control scheme is proposed to drive the system to obey such constraint in this section. That is, a problem of approximate constraint following control is addressed. This should open a new door for motion control of the CAV system.

First, for constraint analysis, we consider the ideal kinematic performance (1) as a *first-order constraint* on vehicle i. Let

$$\mathcal{G}_i(q) := -\sum_{j=1, j\neq i}^N \frac{\partial G_{ij}}{\partial q_i}(q_i, q_j) \tag{32}$$

where $q = [q_1^T, q_2^T, \ldots, q_N^T]^T, q \in \mathbf{R}^{2N}$. By introducing (32), the constraint (1) can be rewritten as

$$\dot{q}_i = \mathcal{G}_i(q). \tag{33}$$

Taking its first-order derivative with respect to t, and denoting the right-hand side of the derivative as φ_i, we obtain the *second-order constraint* as

$$\ddot{q}_i = \varphi_i(q, \dot{q}, t). \tag{34}$$

Note that the constraint (34) is consistent [27]; hence, for a given configuration q_i and q_j of the system, there is at least one acceleration $\ddot{q}_i$ that satisfies the constraint. With the first order constraint (33), define a *constraint-following error* as

$$\beta_i := \dot{q}_i - \mathcal{G}_i \tag{35}$$

where $\beta_i = [\beta_i^x\ \beta_i^y]^T$. It can be seen as a measure of the degree to which the desired constraint is followed: for perfect constraint following case, $\beta_i \equiv 0$. For other cases, its magnitude stands for the extent of constraint violation that is excepted to be the closer to 0, the better. In this sense, $\beta_i = 0$ is actually an ideal condition that is almost impossible to achieve, while $\beta_i \to 0$ is the actual *control objective*.

Taking the first-order derivative of β_i with respect to t, we obtain the β_i-dynamics as

$$\dot{\beta}_i = \ddot{q}_i - \varphi_i. \tag{36}$$

With (24), it can be rewritten as

$$\begin{aligned}\dot{\beta}_i = {} & Q_i^{-1}M_i^{-1}(\tau_i - C_i - F_i) - Q_i^{-1}H_i\\ & - Q_i^{-1}M_{i-1}^{-1}(\tau_{i-1} - C_{i-1} - F_{i-1}) - \varphi_i.\end{aligned} \tag{37}$$

Second, for uncertainty handling, we decompose M_i, C_i, and F_i as follows:

$$M_i(X_i, \sigma_i, t) = \bar{M}_i(X_i, t) + \Delta M_i(X_i, \sigma_i, t) \tag{38}$$

$$C_i\left(X_i, \dot{X}_i, \sigma_i, t\right) = \bar{C}_i\left(X_i, \dot{X}_i, t\right) + \Delta C_i\left(X_i, \dot{X}_i, \sigma_i, t\right) \tag{39}$$

$$F_i(X_i, \dot{X}_i, \sigma_i, t) = \bar{F}_i(X_i, \dot{X}_i, t) + \Delta F_i(X_i, \dot{X}_i, \sigma_i, t). \quad (40)$$

Here, $\bar{M}_i, \bar{C}_i$, and $\bar{F}_i$ are the "nominal" portions, and $\Delta M_i, \Delta C_i$, and ΔF_i are the uncertain portions. Suppose $\bar{M}_i$ is symmetric and positive definite and the functions $\bar{M}_i(\cdot), \Delta M_i(\cdot), \bar{C}_i(\cdot), \Delta C_i(\cdot), \bar{F}_i(\cdot)$, and $\Delta F_i(\cdot)$ are all continuous. Let

$$D_i(X_i, \sigma_i, t) \coloneqq M_i^{-1}(X_i, \sigma_i, t) \quad (41)$$
$$\bar{D}_i(X_i, t) \coloneqq \bar{M}_i^{-1}(X_i, t) \quad (42)$$
$$\Delta D_i(X_i, \sigma_i, t) \coloneqq D_i(X_i, \sigma_i, t) - \bar{D}_i(X_i, t) \quad (43)$$
$$E_i(X_i, \sigma_i, t) \coloneqq \bar{M}_i(X_i, t) M_i^{-1}(X_i, \sigma_i, t) - I_i. \quad (44)$$

Therefore

$$\Delta D_i(X_i, \sigma_i, t) = \bar{D}_i(X_i, t) E_i(X_i, \sigma_i, t). \quad (45)$$

Based on the decomposition, with (24), we obtain the *nominal* system as

$$\bar{M}_i Q_i \ddot{q}_i + \bar{C}_i + \bar{F}_i + \bar{M}_i H_i + \bar{M}_i \bar{D}_{i-1}(\tau_{i-1} - \bar{C}_{i-1} - \bar{F}_{i-1}) = \tau_i. \quad (46)$$

Theorem 2 (Udwadia and Kalaba [31]): Consider the CAV swarm system (7) or (24) without uncertainty and the constraint (1). The constraint force

$$Q_i^c = \bar{M}_i Q_i \varphi_i + \bar{C}_i + \bar{F}_i + \bar{M}_i H_i + \bar{M}_i \bar{D}_{i-1}(\tau_{i-1} - \bar{C}_{i-1} - \bar{F}_{i-1}) \quad (47)$$

observes Lagrange's form of d'Alembert's principle and renders the system to meet the constraint.

Remark 7: With a control $\tau_i = Q_i^c$, the *nominal* system can meet the desired constraint as (1) strictly (i.e., render *perfect* constraint following). As for the entire uncertain system (7) or (24), a more realistic control is needed.

Following analysis is continued for control design of the entire uncertain system (7) or (24). Upon decomposition, the β-dynamics can be reexpressed as

$$\begin{aligned}\dot{\beta}_i = {} & Q_i^{-1}\bar{D}_i(\tau_i - \bar{C}_i - \bar{F}_i) - Q_i^{-1}H_i \\ & - Q_i^{-1}\bar{D}_{i-1}(\tau_{i-1} - \bar{C}_{i-1} - \bar{F}_{i-1}) - \varphi_i \\ & + Q_i^{-1}\bar{D}_i\big[E_i(\tau_i - C_i - F_i) - (\Delta C_i + \Delta F_i) \\ & \quad + \bar{M}_i \Delta D_{i-1}(\tau_{i-1} - C_{i-1} - F_{i-1}) \\ & \quad + \bar{M}_i \bar{D}_{i-1}(\Delta C_{i-1} + \Delta F_{i-1})\big]. \end{aligned} \quad (48)$$

Assumption 1: There exist a constant $\kappa_i \in (0, \infty)$ and a function $f_i(\kappa_i, \cdot) : \mathbf{R}^2 \times \mathbf{R} \to \mathbf{R}^2$ such that there are a Lyapunov function $V_i(\cdot) : \mathbf{R}^2 \times \mathbf{R} \to \mathbf{R}_+$, and strictly increasing functions $\gamma_i^l(\cdot) : \mathbf{R}_+ \to \mathbf{R}_+$ satisfying

$$\gamma_i^l(0) = 0, \quad \lim_{r_i \to \infty} \gamma_i^l(r_i) = \infty, \quad l = 1, 2, 3 \quad (49)$$

such that for all $(\kappa_i, \beta_i, q_i, \dot{q}_i, t) \in (0, \infty) \times \mathbf{R}^2 \times \mathbf{R}^2 \times \mathbf{R}^2 \times \mathbf{R}$

$$\gamma_i^1(\|\beta_i\|) \le V_i(\beta_i, t) \le \gamma_i^2(\|\beta_i\|) \quad (50)$$
$$\frac{\partial V_i(\beta_i, t)}{\partial t} + \frac{\partial^T V_i(\beta_i, t)}{\partial \beta_i} f_i(\kappa_i, \beta_i, t) \le -\kappa_i \gamma_i^3(\|\beta_i\|). \quad (51)$$

We now choose

$$p_i^1 = \bar{M}_i Q_i (f_i + \varphi_i) + \bar{C}_i + \bar{F}_i + \bar{M}_i H_i + \bar{M}_i \bar{D}_{i-1}(\tau_{i-1} - \bar{C}_{i-1} - \bar{F}_{i-1}). \quad (52)$$

Theorem 3: Subject to Assumption 1, the control $\tau_i = p_i^1$ renders

$$Q_i^{-1}\bar{D}_i(\tau_i - \bar{C}_i - \bar{F}_i) - Q_i^{-1}H_i - Q_i^{-1}\bar{D}_{i-1}(\tau_{i-1} - \bar{C}_{i-1} - \bar{F}_{i-1}) - \varphi_i = f_i. \quad (53)$$

Proof: Using $\tau_i = p_i^1$ as (52) in the left-hand side of (53), we have

$$\begin{aligned} & Q_i^{-1}\bar{D}_i\big[\bar{M}_i Q_i (f_i + \varphi_i) + \bar{C}_i + \bar{F}_i + \bar{M}_i H_i \\ & \quad + \bar{M}_i \bar{D}_{i-1}(\tau_{i-1} - \bar{C}_{i-1} - \bar{F}_{i-1}) - \bar{C}_i - \bar{F}_i\big] - Q_i^{-1}H_i \\ & - Q_i^{-1}\bar{D}_{i-1}(\tau_{i-1} - \bar{C}_{i-1} - \bar{F}_{i-1}) - \varphi_i \\ & = f_i + \varphi_i - \varphi_i \\ & = f_i. \end{aligned} \quad (54)$$

■

Assumption 2: There exists a (possibly unknown) constant $\rho_i^E > -1$ such that for all $(X_i, t) \in \mathbf{R}^2 \times \mathbf{R}$

$$\frac{1}{2} \min_{\sigma_i \in \Sigma_i} \lambda_m\big(E_i(X_i, \sigma_i, t) + E_i^T(X_i, \sigma_i, t)\big) \ge \rho_i^E \quad (55)$$

where $\lambda_m(\cdot)$ denotes the minimum eigenvalue of the concerned matrix.

Remark 8: The constant ρ_i^E is generally unknown, since the uncertainly bound Σ_i is unknown. In the special case, when no uncertainty exists, $M_i = \bar{M}_i$, $E_i = 0$, then one can choose $\rho_i^E = 0$.

Assumption 3:

1) There exist an unknown constant vector $\alpha_i \in (0, \infty)^{k_i}$ and a known function $\Pi_i(\cdot) : (0, \infty)^{k_i} \times \mathbf{R}^2 \times \mathbf{R}^2 \times \mathbf{R}^2 \times \mathbf{R}^2 \times \mathbf{R} \to \mathbf{R}_+$ such that for all $(q_i, \dot{q}_i, X_{i-1}, \dot{X}_{i-1}, t) \in \mathbf{R}^2 \times \mathbf{R}^2 \times \mathbf{R}^2 \times \mathbf{R}^2 \times \mathbf{R}$, $\sigma_i \in \Sigma_i$

$$\begin{aligned} & \Big\| E_i\big(p_i^1 - C_i - F_i\big) - (\Delta C_i + \Delta F_i) \\ & \quad + \bar{M}_i \Delta D_{i-1}(\tau_{i-1} - C_{i-1} - F_{i-1}) \\ & \quad + \bar{M}_i \bar{D}_{i-1}(\Delta C_{i-1} + \Delta F_{i-1}) \Big\| \\ & \le \Pi_i(\alpha_i, q_i, \dot{q}_i, X_{i-1}, \dot{X}_{i-1}, t). \end{aligned} \quad (56)$$

2) For each $(q_i, \dot{q}_i, X_{i-1}, \dot{X}_{i-1}, t) \in \mathbf{R}^2 \times \mathbf{R}^2 \times \mathbf{R}^2 \times \mathbf{R}^2 \times \mathbf{R}$, the function $\Pi_i(\cdot, q_i, \dot{q}_i, X_{i-1}, \dot{X}_{i-1}, t) : (0, \infty)^{k_i} \to \mathbf{R}_+$ is: a) C^1; b) concave; that is, for any $\alpha_i^{1,2} \in (0, \infty)^{k_i}$

$$\begin{aligned} & \Pi_i\big(\alpha_i^1, q_i, \dot{q}_i, X_{i-1}, \dot{X}_{i-1}, t\big) - \Pi_i\big(\alpha_i^2, q_i, \dot{q}_i, X_{i-1}, \dot{X}_{i-1}, t\big) \\ & \le \frac{\partial \Pi_i}{\partial \alpha_i}\big(\alpha_i^2, q_i, \dot{q}_i, X_{i-1}, \dot{X}_{i-1}, t\big)\big(\alpha_i^1 - \alpha_i^2\big) \end{aligned} \quad (57)$$

and c) nondecreasing with respect to each component of its argument α_i.

We now propose the following control:

$$\tau_i = p_i^1 + p_i^2 \quad (58)$$

with p_i^1 as (52) and p_i^2 as

$$p_i^2 = -\lambda_i \bar{D}_i Q_i^{-1} \frac{\partial V_i}{\partial \beta_i} \Pi_i^2 \quad (59)$$

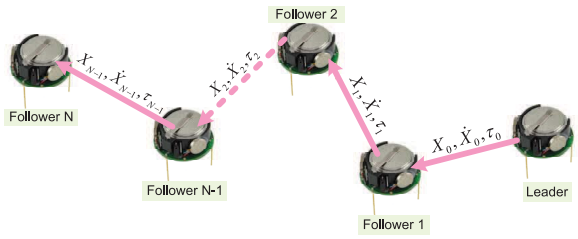

Fig. 2. Information flow topology of the CAVs: PF.

where the scalar $\lambda_i > 0$ is constant design parameter. The parameter $\hat{\alpha}_i$ in the function $\Pi_i(\hat{\alpha}_i, \cdot)$ is governed by the following leakage-type adaptive law:

$$\dot{\hat{\alpha}}_i = \frac{1}{2}k_i^1 \frac{\partial^T \Pi_i}{\partial \alpha_i}\left\| \frac{\partial^T V_i}{\partial \beta_i} Q_i^{-1}\bar{D}_i \right\| - k_i^2 \hat{\alpha}_i \tag{60}$$

where the scalars $k_i^1, k_i^2 > 0$ are design parameters.

Remark 9: According to (56), α_i shows the comprehensive effect of uncertainty on system performance; hence, it is uncertain. The proposed adaptive law as (60) is used to estimate such comprehensive effect online. The control p_i^2 is the adaptive robust action based on the adaptive parameter $\hat{\alpha}_i$, with which the controlled system can resist the effects of uncertainty.

Remark 10: From (52) and (59), it can be seen that besides their own information, each vehicle only needs to know information of the preceding vehicle for control design; hence, the proposed controller is a distributed one. That is to say, in the proposed formation control scheme, each vehicle is required to communicate with only the former one and the latter one. Shown as Fig. 2, the information flow topology of the CAVs is in type of predecessor following (PF) [32].

Theorem 4: Let $\delta_i := [\beta_i^T \ (\hat{\alpha}_i - \alpha_i)^T]^T \in \mathbf{R}^{2+k_i}$ and $\delta(t) := [\delta_1^T(t) \ \delta_2^T(t) \cdots \delta_N^T(t)]^T \in \mathbf{R}^{\sum_{i=1}^N (2+k_i)}$. Consider system (7) or (24). Subject to Assumptions 1–3, the control (58) renders the following performance.

1) *Uniform Boundedness:* For any $r > 0$, there is a $d(r) < \infty$ such that if $\|\delta(t_0)\| \le r$, then $\|\delta(t)\| \le d(r)$ for all $t \ge t_0$.
2) *Uniform Ultimate Boundedness:* For any $r > 0$ with $\|\delta(t_0)\| \le r$, there exist a $\underline{d} > 0$ and a time $T(\bar{d}, r) < \infty$ such that $\|\delta(t)\| \le \bar{d}$ for any $\bar{d} > \underline{d}$ as $t \ge t_0 + T(\bar{d}, r)$.

Proof: Choose $\mathcal{V} = \sum_{i=1}^N \mathcal{V}_i$ as the Lyapunov function candidate, where

$$\mathcal{V}_i(\beta_i, \hat{\alpha}_i - \alpha_i, t) = V_i(\beta_i, t) + \left(k_i^1\right)^{-1}(\hat{\alpha}_i - \alpha_i)^T(\hat{\alpha}_i - \alpha_i) \tag{61}$$

and $V_i(\cdot)$ is subject to Assumption 1. The Lyapunov derivative for the system (24) is given by

$$\dot{\mathcal{V}} = \sum_{i=1}^N \dot{\mathcal{V}}_i. \tag{62}$$

Taking the derivative of (61) yields

$$\dot{\mathcal{V}}_i = \underbrace{\frac{\partial V_i}{\partial t} + \frac{\partial^T V_i}{\partial \beta_i}\dot{\beta}_i}_{=\dot{V}_i} + 2\left(k_i^1\right)^{-1}(\hat{\alpha}_i - \alpha_i)^T \dot{\hat{\alpha}}_i. \tag{63}$$

We first focus on $\dot{V}_i$. Recalling $\dot{\beta}_i$ as (48), we have

$$\begin{aligned}\dot{V}_i = \frac{\partial V_i}{\partial t} &+ \frac{\partial^T V_i}{\partial \beta_i}\Big[Q_i^{-1}\bar{D}_i\left(p_i^1 - \bar{C}_i - \bar{F}_i\right) - Q_i^{-1}H_i \\ &- Q_i^{-1}\bar{D}_{i-1}\left(\tau_{i-1} - \bar{C}_{i-1} - \bar{F}_{i-1}\right) - \varphi_i\Big] \\ &+ \frac{\partial^T V_i}{\partial \beta_i}Q_i^{-1}\bar{D}_i\Big[E_i\left(p_i^1 - C_i - F_i\right) - (\Delta C_i + \Delta F_i) \\ &+ \bar{M}_i\Delta D_{i-1}(\tau_{i-1} - C_{i-1} - F_{i-1}) \\ &+ \bar{M}_i\bar{D}_{i-1}(\Delta C_{i-1} + \Delta F_{i-1})\Big] \\ &+ \frac{\partial^T V_i}{\partial \beta_i}Q_i^{-1}\bar{D}_i p_i^2 + \frac{\partial^T V_i}{\partial \beta_i}Q_i^{-1}\bar{D}_i E_i p_i^2.\end{aligned} \tag{64}$$

With (53) and (51), we have

$$\begin{aligned}&\frac{\partial V_i}{\partial t} + \frac{\partial^T V_i}{\partial \beta_i}\Big[Q_i^{-1}\bar{D}_i\left(p_i^1 - \bar{C}_i - \bar{F}_i\right) - Q_i^{-1}H_i \\ &\qquad - Q_i^{-1}\bar{D}_{i-1}\left(\tau_{i-1} - \bar{C}_{i-1} - \bar{F}_{i-1}\right) - \varphi_i\Big] \\ &= \frac{\partial V_i}{\partial t} + \frac{\partial^T V_i}{\partial \beta_i}f_i \\ &\le -\kappa_i\gamma_i^3(\|\beta_i\|).\end{aligned} \tag{65}$$

With (56), we have

$$\begin{aligned}&\underbrace{\frac{\partial^T V_i}{\partial \beta_i}Q_i^{-1}\bar{D}_i}_{=:\phi_i^T}\Big[E_i\left(p_i^1 - C_i - F_i\right) - (\Delta C_i + \Delta F_i) \\ &\qquad + \bar{M}_i\Delta D_{i-1}(\tau_{i-1} - C_{i-1} - F_{i-1}) \\ &\qquad + \bar{M}_i\bar{D}_{i-1}(\Delta C_{i-1} + \Delta F_{i-1})\Big] \\ &\le \|\phi_i\|\Pi_i(\alpha_i, \cdot).\end{aligned} \tag{66}$$

With (59), we have

$$\frac{\partial^T V_i}{\partial \beta_i}Q_i^{-1}\bar{D}_i p_i^2 = -\lambda_i\|\phi_i\|^2\Pi_i^2(\hat{\alpha}_i, \cdot). \tag{67}$$

Note that $\bar{D}_i$ and Q_i are diagonal matrices. With (55), we further have

$$\begin{aligned}&\frac{\partial^T V_i}{\partial \beta_i}Q_i^{-1}\bar{D}_i E_i p_i^2 \\ &= -\frac{1}{2}\lambda_i \underbrace{\frac{\partial^T V_i}{\partial \beta_i}Q_i^{-1}\bar{D}_i}_{=\phi_i}\left(E_i + E_i^T\right)\underbrace{\bar{D}_i Q_i^{-1}\frac{\partial V_i}{\partial \beta_i}}_{=\phi_i^T}\Pi_i^2(\hat{\alpha}_i, \cdot) \\ &\le -\frac{1}{2}\lambda_i\phi_i\lambda_m\left(E_i + E_i^T\right)\phi_i^T\Pi_i^2(\hat{\alpha}_i, \cdot) \\ &\le -\lambda_i\rho_i^E\|\phi_i\|^2\Pi_i^2(\hat{\alpha}_i, \cdot).\end{aligned} \tag{68}$$

Introducing (65)–(68) into (64), we have

$$\begin{aligned}\dot{V}_i \le &-\kappa_i\gamma_i^3(\|\beta_i\|) + \|\phi_i\|\Pi_i(\alpha_i, \cdot) \\ &- \lambda_i\left(1 + \rho_i^E\right)\|\phi_i\|^2\Pi_i^2(\hat{\alpha}_i, \cdot).\end{aligned} \tag{69}$$

We then focus on the second term of the left-hand side of (63). Recalling $\hat{\alpha}_i$ as (60), we have

$$\begin{aligned}
&2\left(k_i^1\right)^{-1}\left(\hat{\alpha}_i-\alpha_i\right)^T\dot{\hat{\alpha}}_i\\
&=\left(\hat{\alpha}_i-\alpha_i\right)^T\frac{\partial^T\Pi_i}{\partial\alpha_i}\left(\hat{\alpha}_i,\cdot\right)\|\phi_i\|-2\left(k_i^1\right)^{-1}k_i^2\left(\hat{\alpha}_i-\alpha_i\right)^T\left(\hat{\alpha}_i-\alpha_i\right)\\
&\quad-2k_i^2\left(\hat{\alpha}_i-\alpha_i\right)^T\alpha_i\\
&\le\left(\hat{\alpha}_i-\alpha_i\right)^T\frac{\partial^T\Pi_i}{\partial\alpha_i}\left(\hat{\alpha}_i,\cdot\right)\|\phi_i\|-\left(k_i^1\right)^{-1}k_i^2\left\|\hat{\alpha}_i-\alpha_i\right\|^2\\
&\quad+\left(k_i^1\right)^{-1}k_i^2\|\alpha_i\|^2. \qquad (70)
\end{aligned}$$

By combining (69) and (70) in (63), we have

$$\begin{aligned}
\dot{\mathcal{V}}_i&\le-\kappa_i\gamma_i^3(\|\beta_i\|)-\left(\hat{\alpha}_i-\alpha_i\right)^T\frac{\partial^T\Pi_i}{\partial\alpha_i}\left(\hat{\alpha}_i,\cdot\right)\|\phi_i\|\\
&\quad+\frac{1}{4\lambda_i\left(1+\rho_i^E\right)}+\left(\hat{\alpha}_i-\alpha_i\right)^T\frac{\partial^T\Pi_i}{\partial\alpha_i}\left(\hat{\alpha}_i,\cdot\right)\|\phi_i\|\\
&\quad-\left(k_i^1\right)^{-1}k_i^2\left\|\hat{\alpha}_i-\alpha_i\right\|^2+\left(k_i^1\right)^{-1}k_i^2\|\alpha_i\|^2\\
&=-\kappa_i\gamma_i^3(\|\beta_i\|)-\left(k_i^1\right)^{-1}k_i^2\left\|\hat{\alpha}_i-\alpha_i\right\|^2\\
&\quad+\underbrace{\frac{1}{4\lambda_i\left(1+\rho_i^E\right)}+\left(k_i^1\right)^{-1}k_i^2\|\alpha_i\|^2}_{=:\zeta_i}\\
&=-\kappa_i\gamma_i^3(\|\beta_i\|)-\left(k_i^1\right)^{-1}k_i^2\left\|\hat{\alpha}_i-\alpha_i\right\|^2+\zeta_i. \qquad (71)
\end{aligned}$$

Recall $\delta_i=[\beta_i^T\ \ (\hat{\alpha}_i-\alpha_i)^T]^T$, and let

$$\hat{\gamma}_i^3(v_i):=\min_{\delta_i}\left\{\kappa_i\gamma_i^3(\|\beta_i\|),\left(k_i^1\right)^{-1}k_i^2\left\|\hat{\alpha}_i-\alpha_i\right\|^2\mid v_i=\|\delta_i\|\right\} \qquad (72)$$

with which we have

$$\dot{\mathcal{V}}_i\le-\hat{\gamma}_i^3(\|\delta_i\|)+\zeta_i. \qquad (73)$$

Recalling (61), we conclude the uniform boundedness and uniform ultimate boundedness of the vehicle i ([33]) as follows.

1) Given any $r_i>0$, with $\|\delta_{0i}\|\le r_i$, where $\delta_{0i}=\delta_i(t_0)$ and t_0 is the initial time, there exists

$$d_i(r_i)=\begin{cases}\left(\left(\gamma_i^1\right)^{-1}\circ\gamma_i^2\right)(r_i), & \text{if } r_i>R_i\\ \left(\left(\gamma_i^1\right)^{-1}\circ\gamma_i^2\right)(R_i), & \text{if } r_i\le R_i.\end{cases} \qquad (74)$$

$$R_i=\left(\gamma_i^3\right)^{-1}(\zeta_i) \qquad (75)$$

such that $\|\delta_i(t)\|\le d_i(r_i)$ for all $t\ge t_0$.

2) Given any $\bar{d}_i$, with

$$\bar{d}_i>\left(\left(\gamma_i^1\right)^{-1}\circ\gamma_i^2\right)(R_i) \qquad (76)$$

we have $\|\delta_i(t)\|\le\bar{d}_i$, for all $t\ge t_0+T_i(\bar{d}_i,r_i)$, with

$$T_i\left(\bar{d}_i,r_i\right)=\begin{cases}0, & \text{if } r_i\le\bar{R}_i\\ \frac{\gamma_i^2(r_i)-\gamma_i^1(\bar{R}_i)}{\gamma_i^3(\bar{R}_i)-\zeta_i}, & \text{otherwise}\end{cases} \qquad (77)$$

$$\bar{R}_i=\left(\left(\gamma_i^2\right)^{-1}\circ\gamma_i^1\right)(\bar{d}_i). \qquad (78)$$

The following analysis is continued for the *global* performance of system (7) or (24). Recalling $\delta=[\delta_1^T\ \delta_2^T\cdots\delta_N^T]^T$, let

$$\begin{aligned}
\gamma_1(v)&:=\min_{\delta}\Big\{\kappa_1\gamma_1^3(\|\beta_1\|)+(k_1^1)^{-1}k_1^2\left\|\hat{\alpha}_1-\alpha_1\right\|^2,\ldots\\
&\qquad\kappa_N\gamma_N^3(\|\beta_N\|)+\left(k_N^1\right)^{-1}k_N^2\left\|\hat{\alpha}_N-\alpha_N\right\|^2\mid v=\|\delta\|\Big\}\\
\gamma_2(v)&:=\max_{\delta}\Big\{\kappa_1\gamma_1^3(\|\beta_1\|)+\left(k_1^1\right)^{-1}k_1^2\left\|\hat{\alpha}_1-\alpha_1\right\|^2,\ldots\\
&\qquad\kappa_N\gamma_N^3(\|\beta_N\|)+\left(k_N^1\right)^{-1}k_N^2\left\|\hat{\alpha}_N-\alpha_N\right\|^2\mid v=\|\delta\|\Big\}.
\end{aligned} \qquad (79)$$

Taking (73) into (62), we have

$$\dot{\mathcal{V}}\le-\sum_{i=1}^N\hat{\gamma}_i^3(\|\delta_i\|)+\sum_{i=1}^N\zeta_i. \qquad (80)$$

Let

$$\gamma_3(v):=\min_{\delta}\left\{\hat{\gamma}_1^3(\|\delta_1\|),\ldots,\hat{\gamma}_N^3(\|\delta_N\|)\mid v=\|\delta\|\right\} \qquad (81)$$

with which we have

$$\begin{aligned}
\dot{\mathcal{V}}&\le-\gamma_3(\|\delta\|)+\sum_{i=1}^N\zeta_i\\
&=:-\gamma_3(\|\delta\|)+\zeta. \qquad (82)
\end{aligned}$$

We conclude the uniform boundedness and uniform ultimate boundedness of the system (7) or (24) ([33]) as follows.

1) Given any $r>0$, with $\|\delta_0\|\le r$, where $\delta_0=\delta(t_0)$ and t_0 is the initial time, there exists

$$d(r)=\begin{cases}\left(\gamma_1^{-1}\circ\gamma_2\right)(r), & \text{if } r>R\\ \left(\gamma_1^{-1}\circ\gamma_2\right)(R), & \text{if } r\le R.\end{cases} \qquad (83)$$

$$R=\gamma_3^{-1}(\zeta) \qquad (84)$$

such that $\|\delta(t)\|\le d(r)$ for all $t\ge t_0$.

2) Given any $\bar{d}$, with

$$\bar{d}>\left(\gamma_1^{-1}\circ\gamma_2\right)(R) \qquad (85)$$

we have $\|\delta(t)\|\le\bar{d}$, for all $t\ge t_0+T(\bar{d},r)$, with

$$T(\bar{d},r)=\begin{cases}0, & \text{if } r\le\bar{R}\\ \frac{\gamma_2(r)-\gamma_1(\bar{R})}{\gamma_3(\bar{R})-\zeta}, & \text{otherwise}\end{cases} \qquad (86)$$

$$\bar{R}=\left(\gamma_2^{-1}\circ\gamma_1\right)(\bar{d}). \qquad (87)$$

The performance is guaranteed. ■

Remark 11: By taking the ideal kinematic performance (1) as constraint on vehicle i, we formulate the control of CAV swarm system as a task of approximative constraint following. The proposed control (58) not only renders the performance of uniform boundedness and uniform ultimate boundedness for individual vehicle i but also renders global one for the entire CAV swarm system.

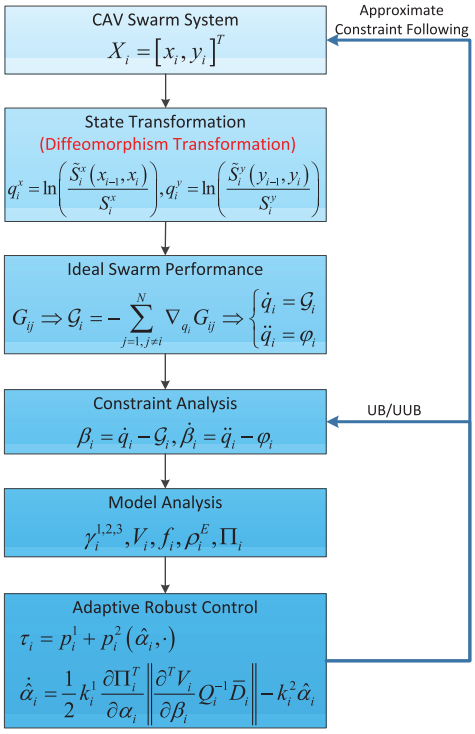

Fig. 3. Design procedure.

VI. Design Procedure

This article propose an adaptive robust formation control scheme for the CAV swarm system by incorporating swarm property, diffeomorphism transformation, and constraint following. Shown as Fig. 3, the design procedure is summarized as follows.

1) Determine the horizontal space measure $\tilde{S}_i^x$ as (10) and the vertical space measure $\tilde{S}_i^y$ as (11), and then formulate the transformed states q_i^x and q_i^y as (16).
2) Formulate the function $G_{ij}(\cdot)$ according to Properties $1-4$ and obtain $\mathcal{G}_i(\cdot)$ according to (32) and $\varphi_i(\cdot)$ according to (34). Define the constraint-following error β_i as (35).
3) Determine $f_i(\kappa_i, \cdot), \gamma_i^{1,2,3}(\cdot), V_i(\cdot)$ according to Assumption 1, ρ_{E_1} according to Assumption 2, and $\Pi_i(\cdot)$ according to Assumption 3.
4) With predetermined $f_i(\kappa_i, \cdot), \varphi_i(\cdot), V_i(\cdot), \Pi_i(\cdot)$, determine the partial controls p_i^1 as (52), p_i^2 as (59) and the adaptive law $\dot{\hat{\alpha}}$ as (60).
5) With predetermined p_i^1 and p_i^2, design the adaptive robust control τ_i according to (58).

Remark 12: The novelty of the proposed method is threefold. First, it solves a more generalized *planar* rather than *linear* formation control problem for CAV swarm system by proposing a 2-D formation control scheme. Second, it can realize compact formation for the concerned CAV swarm system by taking the ideal swarm performance as a desired constraint and formulating a constraint-following framework. Third, it considers both collision avoidance and time-varying uncertainty in the process of formation control design.

VII. Application: Formation Marching and Cooperative Operation

In this section, we consider an application of the proposed control scheme for formation marching and cooperative operation of the CAV swarm system. That is, it expects a control to drive the CAV swarm system close to a predetermined target object in a compact formation, and go around it for cooperative operation purposes, such as collaborative transportation, siege, cooperative reconnaissance, etc.

A. System Model and Constraint Analysis

A CAV swarm system usually contains three to six vehicles. As a most complicated case, we consider a CAV swarm system with seven vehicles (including one virtual leader and six followers) shown as in Fig. 4. It expects the CAV swarm system to reach a target object and go around it. The equation motion of the (virtual) leader is expressed as (6) and the equation motion of the followers is expressed as (7), in which the inertia matrices can be detailed as $M_i = \text{diag}\{m_i\}$ $(i = 0, 1, 2, 3, 4, 5, 6)$. m_i is the mass of vehicle i. Ignoring the aerodynamic drag force and external disturbances in y direction, the terms of C_i and F_i in (7) can be detailed as $C_i = [C_i^x \ 0]^T$ and $F_i = [F_i^x \ 0]^T$, in which C_i^x is the aerodynamic drag force in x direction and can be expressed as $C_i^x = c_i|\dot{x}_i|\dot{x}_i$. c_i is the aerodynamic drag coefficient and F_i^x is the external disturbances in x direction.

As the load in each vehicle is uncertain, and the aerodynamic drag force as well as the external disturbance are inevitable, we suppose the mass m_i, the aerodynamic drag coefficient c_i, and the disturbance F_i^x are uncertain: $m_i = \bar{m}_i + \Delta m_i(t)$, $c_i = \bar{c}_i + \Delta c_i(t)$, $F_i^x = \bar{F}_i^x + \Delta F_i^x(t)$. To evaluate the robustness of the proposed controller, we choose *high-frequency uncertainties* as $\Delta m_i(t) = 40\sin(10t)$, $\Delta c_i(t) = \sin(10t)$, and $\Delta F_i^x(t) = 15\sin(10t)$ as interference signal. The later simulation results show that the controller can resist such strong uncertainty interference; hence, has strong robustness. What is more, in order to further verify the uncertainty resistance ability of the proposed controller, we choose amplified uncertainty as $\Delta m_i(t) = 80\sin(t)$, $\Delta c_i(t) = 10\sin(t)$, and $\Delta F_i^x(t) = 30\sin(t)$, and a set of low-frequency uncertainty as $\Delta m_i(t) = 40\sin(t)$, $\Delta c_i(t) = \sin(t)$, and $\Delta F_i^x(t) = 15\sin(t)$ for comparison.

For constraint analysis, we choose the function $G_{ij}(\cdot)$ as

$$G_{ij} = -\left(\|q_i - q_j\|^2 + a\right)^{\frac{1}{2}} + \frac{1}{2}\|q_i - q_j\|^2 \tag{88}$$

where $a \geq 0$ is a constant scalar. Taking the derivative of it with respect to q^i, we have

$$\frac{\partial G_{ij}}{\partial q_i} = \left[1 - \left(\|q_i - q_j\|^2 + a\right)^{-\frac{1}{2}}\right](q_i - q_j). \tag{89}$$

Recalling (32), we have

$$\mathcal{G}_i = \sum_{j=1, j\neq i}^{6} \left[\left(\|q_i - q_j\|^2 + a\right)^{-\frac{1}{2}} - 1\right](q_i - q_j). \tag{90}$$

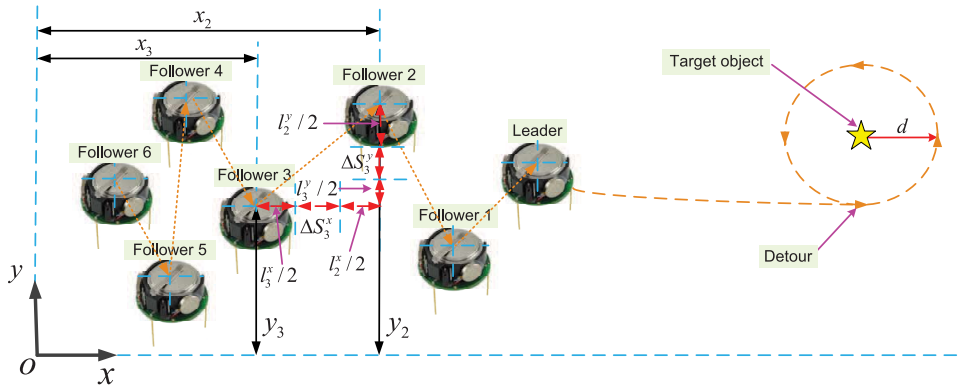

Fig. 4. CAV swarm system with 6 vehicles.

With (90) and (35), we have

$$\beta_i = \dot{q}_i - \sum_{j=1, j\neq i}^{6} \left[\left(\|q_i - q_j\|^2 + a \right)^{-\frac{1}{2}} - 1 \right] (q_i - q_j). \quad (91)$$

Recalling (34), and taking the derivative of (90) with respect to t, we have

$$\varphi_i = \sum_{j=1, j\neq i}^{6} \left\{ -\left(\|q_i - q_j\|^2 + a \right)^{-\frac{3}{2}} (q_i - q_j)^T (\dot{q}_i - \dot{q}_j) \times (q_i - q_j) + \left[\left(\|q_i - q_j\|^2 + a \right)^{-\frac{1}{2}} - 1 \right] (\dot{q}_i - \dot{q}_j) \right\}. \quad (92)$$

B. Assumption Verification

We now focus on the verification of Assumptions 1–3. First, for Assumption 1, we consider a Lyapunov function as $V_i(\beta_i) = \beta_i^T P_i \beta_i$, with $P_i > 0$, $P_i \in \mathbf{R}^{2\times 2}$, and $f_i(\kappa_i, \beta_i) = -\epsilon_i \kappa_i \beta_i$, $\epsilon_i > 0$, and then select the corresponding functions $\gamma_i^1(\|\beta_i\|) = \lambda_m(P_i)\|\beta_i\|^2$, $\gamma_i^2(\|\beta_i\|) = \lambda_M(P_i)\|\beta_i\|^2$ and $\gamma_i^3 = \epsilon_i \lambda_M(P_i)\|\beta_i\|^2$.

Second, for Assumption 2, with (55), we have $E_i = \bar{M}_i M_i^{-1} - I_i$. As $M_i > 0$, $\bar{M}_i > 0$, $\bar{M}_i M_i^{-1} > 0$; hence, $(1/2)\min_{\sigma_i \in \Sigma_i} \lambda_m(E_i + E_i^T) \geq \rho_i^E > -1$, such that (55) is satisfied.

Third, as all the entries in M_i, C_i, and F_i are either constant, trigonometric in positions, velocities, or quadratic in velocities, Assumption 3 is met by choosing

$$\Pi_i(\alpha_i, \dot{X}_i) = \alpha_i^1 \|\dot{X}_i\|^2 + \alpha_i^2 \|\dot{X}_i\| + \alpha_i^3 \quad (93)$$
$$\leq \alpha_i \left(\|\dot{X}_i\|^2 + 2\|\dot{X}_i\| + 1 \right) \quad (94)$$
$$= \alpha_i \left(\|\dot{X}_i\| + 1 \right)^2 \quad (95)$$
$$=: \alpha_i \hat{\Pi}_i(\dot{X}_i) \quad (96)$$

where $\alpha_i^{1,2,3} > 0$ are unknown constant parameters and $\alpha_i = \max\{\alpha_i^1, \alpha_i^2/2, \alpha_i^3\}$. Here, $\alpha_i^1 \|\dot{X}_i\|^2$, $\alpha_i^2 \|\dot{X}_i\|$, and α_i^3 are, respectively, determined according to the structures of the quadratic in velocities, the velocities, and the constant as well as the trigonometric in positions.

C. Control Design

The leader vehicle is actually a virtual one and we number it as vehicle 0. As it is virtual, we take it as a moving particle in our design procedure. First, for the leader (i.e., the vehicle 0), a control τ_0 is designed to drive it close to a given position (x_d, y_d), where x_d, y_d are constants. By this, under the guidance of the leader, the followers can also close to the given position with the later designed control. Define the *tracking error* as

$$e := (x_0 - x_d)^2 + (y_0 - y_d)^2 - d^2. \quad (97)$$

Taking the derivative of it with respect to t, we have

$$\dot{e} = 2(x_0 - x_d)\dot{x}_0 + 2(y_0 - y_d)\dot{y}_0 \quad (98)$$
$$\ddot{e} = 2(x_0 - x_d)\ddot{x}_0 + 2(y_0 - \bar{y}_d)\ddot{y}_0 + 2\dot{x}_0^2 + 2\dot{y}_0^2. \quad (99)$$

We consider the leader is constrained by $\dot{e} + l_0 e = 0, l_0 > 0$ is scalar, that is

$$2(x_0 - x_d)\dot{x}_0 + 2(y_0 - y_d)\dot{y}_0 + l_0 \left[(x_0 - x_d)^2 + (y_0 - y_d)^2 - d^2 \right] = 0. \quad (100)$$

Taking differentiation, we have

$$2(x_0 - x_d)\ddot{x}_0 + 2(y_0 - \bar{y}_d)\ddot{y}_d + 2\dot{x}_0^2 + 2\dot{y}_0^2 + l_0 \left[2(x_0 - x_d)\dot{x}_0 + 2(y_0 - y_d)\dot{y}_0 \right]. \quad (101)$$

We can write (100) and (101) in the form of matrix as

$$\underbrace{\left[2(x_0 - \bar{x}_d) \;\; 2(y_0 - \bar{y}_d) \right]}_{=:A} \begin{bmatrix} \dot{x}_0 \\ \dot{y}_0 \end{bmatrix} = \underbrace{-l_0 \left[(x_0 - x_d)^2 + (y_0 - y_d)^2 \right]}_{=:c} \quad (102)$$

and

$$\underbrace{\left[2(x_0 - \bar{x}_d) \;\; 2(y_0 - \bar{y}_d) \right]}_{=:A} \begin{bmatrix} \ddot{x}_0 \\ \ddot{y}_0 \end{bmatrix} = \underbrace{-2\dot{x}_0^2 - 2\dot{y}_0^2 - l_0 \left[2(x_0 - x_d)\dot{x}_0 + 2(y_0 - y_d)\dot{y}_0 \right]}_{=:b}. \quad (103)$$

According to [17], we then design τ_0 as

$$\tau_0 = M_0^{1/2} \left(A M_0^{-1/2} \right)^+ b. \quad (104)$$

TABLE I
PARAMETER SETTING

Parameter	Value	Parameter	Value
$m_0(kg)$	1	$\bar{m}_{1,2,3,4,5,6}(kg)$	1200
$l^x_{0,1,2,3,4,5,6}(m)$	5	$l^y_{0,1,2,3,4,5,6}(m)$	5
$\bar{S}^x_{1,2,3,4,5,6}(m)$	5	$\bar{S}^y_{1,2,3,4,5,6}(m)$	5
$\bar{F}^x_{1,2,3,4,5,6}(N)$	200	$\bar{c}_{1,2,3,4,5,6}$	3
(x_d, y_d)	(0,0)	l_0	0.5
$\kappa_{1,2,3,4,5,6}$	10	$\lambda_{1,2,3,4,5,6}$	1
$\epsilon_{1,2,3,4,5,6}$	1	$P_{1,2,3,4,5,6}$	$I_{2\times 2}$
$k_{11,21,31,41,51,61}$	0.01	$k_{12,22,32,42,52,62}$	1
a	0.5	–	–

Second, for the follower i (i.e., the vehicle i), we design a control τ_i according to (58). As we choose $V_i(\beta_i) = \beta_i^T P_i \beta_i$, $\partial V_i/\partial \beta_i = 2P_i\beta_i$. Taking it and the predetermined $f_i = -\epsilon_i\kappa_i\beta_i$, $\beta_i(\cdot)$ as (91), $\varphi_i(\cdot)$ as (92), and $\Pi_i(\cdot)$ as (93) into (52) and (59), we have

$$\tau_i = p_i^1 + p_i^2 \tag{105}$$

with

$$\begin{aligned} p_i^1 = {} & \bar{M}_i Q_i(-\epsilon_i\kappa_i\beta_i + \varphi_i) + \bar{C}_i + \bar{F}_i + \bar{M}_i H_i \\ & + \bar{M}_i\bar{D}_{i-1}\left(\tau_{i-1} - \bar{C}_{i-1} - \bar{F}_{i-1}\right) \end{aligned} \tag{106}$$

and

$$p_i^2 = -2\hat{\alpha}_i^2\lambda_i\bar{D}_i Q_i^{-1} P_i\beta_i\hat{\Pi}_i^2 \tag{107}$$

in which $\hat{\alpha}_i$ is determined by

$$\dot{\hat{\alpha}}_i = k_i^1\hat{\Pi}_i\left\|\beta_i^T P_i Q_i^{-1}\bar{D}_i\right\| - k_i^2\hat{\alpha}_i. \tag{108}$$

D. Simulation

For simulation, we set the parameters as in Table I. Note that there mainly are two types of parameters in the simulation: one type is the modeling parameters of the CAV swarm system and the other type is the design parameters. As for the modeling parameters, they can be selected as arbitrary constants that correspond to their actual physical meaning. As for the design parameters, l_0, a is constraint design parameters and can be selected as any scalars $l_0 > 0$, $a \geq 0$; $k_{11,21,31,41,51,61}$ and $k_{12,22,32,42,52,62}$ are design parameters of adaptive law and can also be selected as any positive scalars; $\epsilon_{1,2,3,4,5,6}, P_{1,2}$ are auxiliary control design parameters and can be selected as any scalars/matrix subject to $\epsilon_{1,2,3,4,5,6} > 0$, $P_{1,2} \in \mathbf{R}^{2\times 2}$, $P_{1,2} > 0$; $\kappa_{1,2,3,4,5,6}$, $\lambda_{1,2,3,4,5,6}$ are control design parameters and can be selected as any positive scalars. We further choose the initial states $x_0(0) = -75$, $\dot{x}_0(0) = 10$, $y_0(0) = -15$, $\dot{y}_0(0) = -10$, $x_1(0) = -90$, $\dot{x}_1(0) = 10.5$, $y_1(0) = -30$, $\dot{y}_1(0) = -10.5$, $x_2(0) = -105$, $\dot{x}_2(0) = 11$, $y_2(0) = -45$, $\dot{y}_2(0) = -11$, $x_3(0) = -120$, $\dot{x}_3(0) = 11.5$, $y_3(0) = -60$, $\dot{y}_3(0) = -11.5$, $x_4(0) = -135$, $\dot{x}_4(0) = 12$, $y_4(0) = -75$, $\dot{y}_4(0) = -12$, $x_5(0) = -150$, $\dot{x}_5(0) = 12.5$, $y_5(0) = -90$, $\dot{y}_5(0) = -12.5$, $x_6(0) = -165$, $\dot{x}_6(0) = 13$, $y_6(0) = -105$, $\dot{y}_6(0) = -3$, and $\hat{\alpha}_{1,2,3,4,5,6}(0) = 1$.

Simulation results are shown in Figs. 5–19. Fig. 5 shows the 3-D trajectories [i.e., the position (x, y) over time t] of the virtual leading vehicle (marked with a red-dotted line) and the six following vehicles. It shows that starting from the initial position, the CAV swarm system arrives to the target object

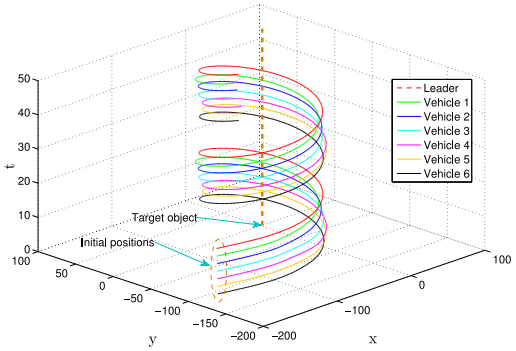

Fig. 5. 3-D trajectories of the vehicles.

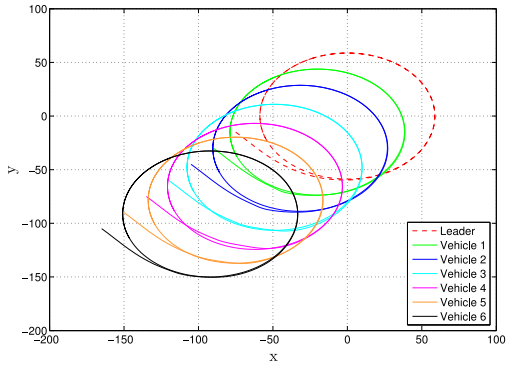

Fig. 6. 2-D trajectories of the vehicles.

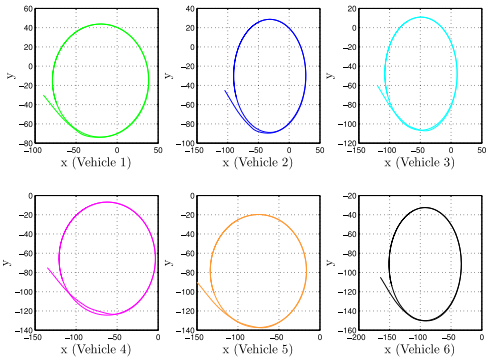

Fig. 7. Individual 2-D trajectories of the vehicles.

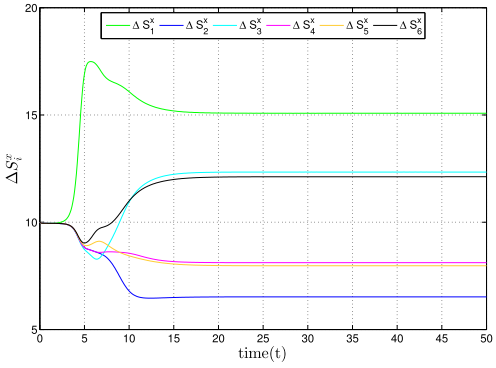

Fig. 8. Histories of the actual horizontal space between vehicle i and its preceding vehicle $i-1$: ΔS_i^x.

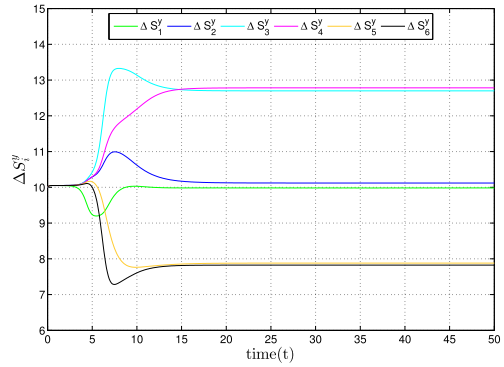

Fig. 9. Histories of the actual vertical space between vehicle i and its preceding vehicle $i-1$: ΔS_i^y.

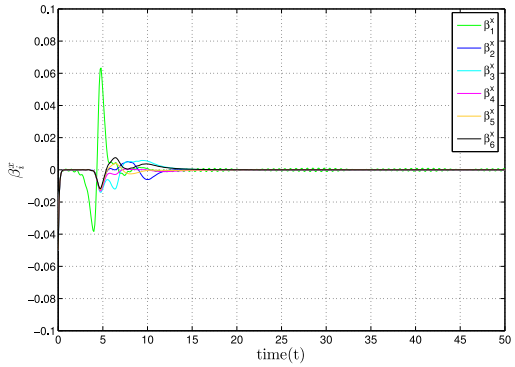

Fig. 10. Histories of the constraint-following errors: β_{xi}.

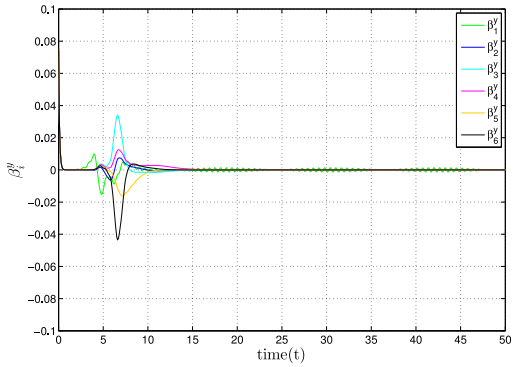

Fig. 11. Histories of the constraint-following errors: β_{yi}.

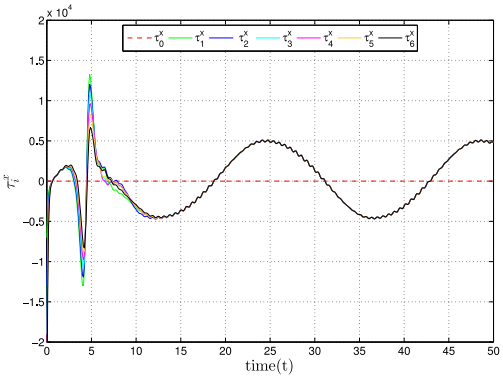

Fig. 12. Control inputs: τ_i^x.

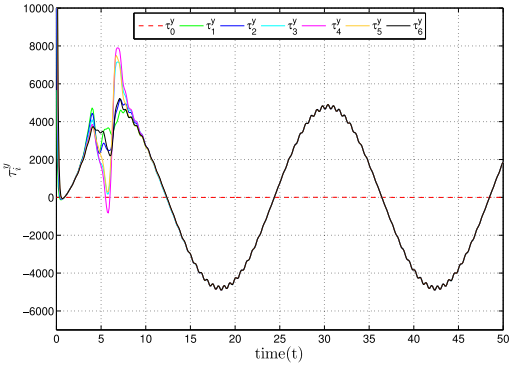

Fig. 13. Control inputs: τ_i^y.

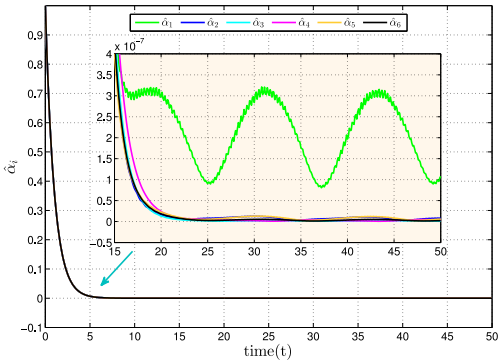

Fig. 14. Histories of the adaptive parameters: $\hat{\alpha}_i$.

and then goes around it under the guidance of the leading vehicle. It can be clearly seen that the seven trajectories are not intersecting at any time and keep at a relatively stable space. It means that the CAV swarm system can avoid collision actively. This actually verifies the effect of state transformation (in Section IV) for collision avoidance. To show the driving route of the vehicles more clearly, their 2-D trajectories [i.e., the position (x, y)] are shown together in Fig. 6 and individually in Fig. 7. It further shows that leading by the virtual vehicle, the CAV swarm system can approach to the target object and drive around it.

Collision avoidance is an important technical target of the CAV swarm system, for which this article does some elaborate efforts in the process of control design. To verify the validity of the proposed method, the histories of the actual horizontal/vertical space ΔS_i^x and ΔS_i^y between vehicle i and its preceding vehicle $i-1$ are especially shown as Figs. 8 and 9. It can be seen that the actual horizontal/vertical space ΔS_i^x and ΔS_i^y are always greater than zero, that is to say, the vehicles will not hit each other any time; thus, the target of collision avoidance is achieved. It further can be seen that the actual horizontal/vertical space ΔS_i^x and ΔS_i^y reach to a relatively stable level between $t = 10$ s and $t = 15$ s, that is to say, the vehicles can maintain a relatively stable formation after $t = 15$ s; thus, the target of formation control is achieved.

The proposed control scheme is formulated based on constraint following, for which constraint-following error β_i is constructed as the core control object. To verify their performances of uniform boundedness and uniform ultimate

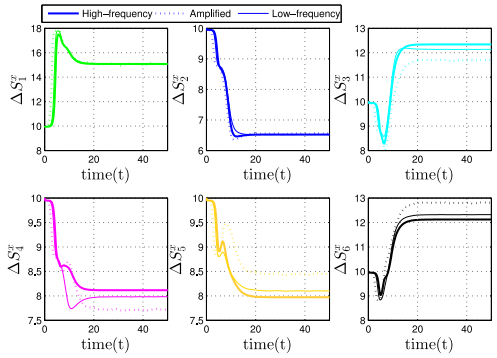

Fig. 15. Comparisons of the actual horizontal space ΔS_i^x with different uncertainties.

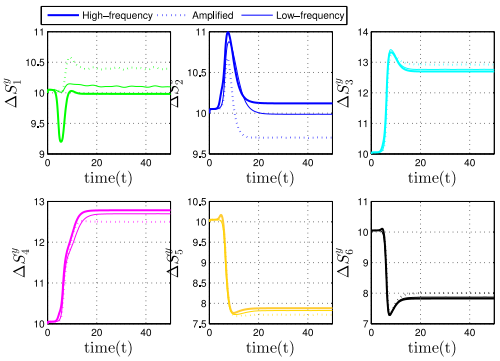

Fig. 16. Comparisons of the actual vertical space ΔS_i^y with different uncertainties.

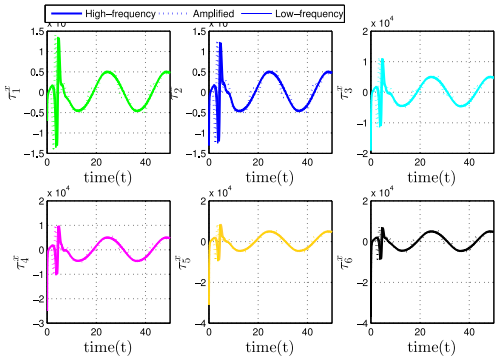

Fig. 17. Comparisons of the control inputs τ_i^x with different uncertainties.

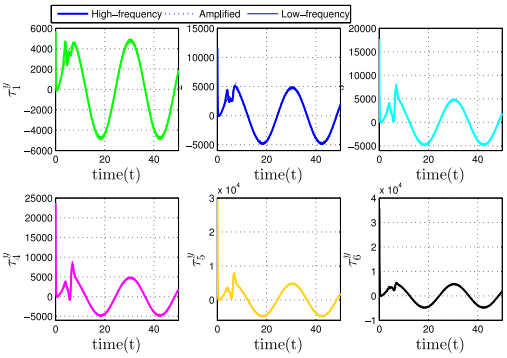

Fig. 18. Comparisons of the control inputs τ_i^y with different uncertainties.

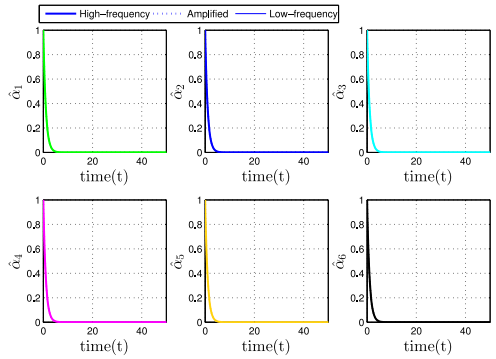

Fig. 19. Comparisons of the adaptive parameters $\hat{\alpha}_i$ with different uncertainties.

boundedness described as Theorem 4, their histories are shown as Figs. 10 and 11. It can be seen that the constraint-following errors β_i^x and β_i^y stay in the range of -0.04–0.065 all the time, and approach to a desirable neighborhood close to 0 before $t = 15$ s. By this, the performances of uniform boundedness and uniform ultimate boundedness are verified. Meanwhile, Figs. 12 and 13 show the corresponding control inputs and Fig. 14 shows the corresponding histories of the adaptive parameters. It can be seen that the control inputs τ_i^x and τ_i^y render to periodic change before $t = 10$ s, and the adaptive parameters $\hat{\alpha}_i$ get close to 0 before $t = 5$ s.

Uncertainty handling is one of the important features of the proposed control scheme. The proposed controller has strong robustness. In order to fully verify the robustness, comparisons between high-frequency uncertainty, amplified uncertainty, and low-frequency uncertainty are carried out and the simulation results are shown in Figs. 15–19. Figs. 15 and 16 show the comparisons of the actual horizontal/vertical space ΔS_i^x and ΔS_i^y between vehicle i and its preceding vehicle $i-1$, and Figs. 14–17 show the comparisons of the corresponding control inputs and adaptive parameters. It can be seen that no matter what kind of uncertainty is involved, the actual horizontal/vertical space ΔS_i^x and ΔS_i^y are always greater than zero and tend to be stable in a certain time, while the larger control input is required for amplified uncertainty. We can conclude that regardless of the complexity and diversity of uncertain interference, the controlled CAV swarm system not only can avoid collision but also can maintain stable space, that is, render compact formation.

VIII. Conclusion

With the development of science and technology, research of CAVs has attracted much attention. This article aims at an adaptive robust formation control scheme for the CAV swarm system. The (possibly fast) time varying but bounded uncertainty is especially considered. The uncertainty bounds are unknown, for which an adaptive law is proposed to estimate their comprehensive effect on system performance online. First, the CAV system is treated as an artificial swarm system. By taking the ideal swarm performance as the desired constraint, the problem of formation control is formulated as a task of constraint following, for which a β-measure is defined as the control object to gauge the constraint following error. Second, state transformation based on diffeomorphism transformation is performed to keep the space measure to be positive for collision avoidance. Third, an adaptive robust control scheme is proposed to render the β-measure to be

uniformly bounded and uniformly ultimately bounded, regardless of the uncertainty. By this, the controlled system is driven to follow the desired constraint approximatively; hence, render the ideal swarm performance. As a result, compact formation is realized. In summary, the most important contribution of this work is doing the first effort that explores formation control for CAV swarm system by incorporating swarm property (for compact formation), diffeomorphism transformation (for collision avoidance), and constraint following (for uncertainty handling).

The main limitation of the proposed control scheme is that it is formulated in a pure view of control and fails to address an overall balance between the control costs and the system performance. However, in practical engineering problems, the control input (such as the output torque of motor) is finite and the system performance does not need to be fully satisfied. It is realistic to adjust the control parameters to achieve an optimal balance between the control cost and the system performance. By this, a problem of optimal parameter design is brought out. Motivated by this, we expect to do further explorations on optimal design in formation control of CAV swarm system in the future.

REFERENCES

[1] C. Zhao, L. Cai, and P. Cheng, "Stability analysis of vehicle platooning with limited communication range and random packet losses," *IEEE Internet Things J.*, vol. 8, no. 1, pp. 262–277, Jan. 2021, doi: 10.1109/JIOT.2020.3004573.

[2] J. Huang, Q. Huang, Y. Deng, and Y.-H. Chen, "Toward robust vehicle platooning with bounded spacing error," *IEEE Trans. Comput.-Aided Design Integr. Circuits Syst.*, vol. 36, no. 4, pp. 562–572, Apr. 2016.

[3] X. Zhao, Y. H. Chen, and H. Zhao, "Robust approximate constraint-following control for autonomous vehicle platoon systems," *Asian J. Control*, vol. 20, no. 4, pp. 1611–1623, 2018.

[4] X. Zhao, J. Ju, F. Dong, Y. H. Chen, L. Zhang, and B. Zhang, "An exponential type control design for autonomous vehicle platoon systems," *Asian J. Control*, vol. 23, no. 2, pp. 1025–1039, 2018, doi: 10.1002/asjc.2279.

[5] F. Dong, X. Zhao, and Y.-H. Chen, "Optimal longitudinal control for vehicular platoon systems: adaptiveness, determinacy, and fuzzy," *IEEE Trans. Fuzzy Syst.*, vol. 29, no. 4, pp. 889–903, Apr. 2021, doi: 10.1109/TFUZZ.2020.2966176.

[6] X. Zhao, H. Zhao, Y. H. Chen, and F. Dong, "Collision avoidance adaptive robust control for autonomous vehicles: motivated by swarm properties," in *Proc. 29th Chin. Control Decis. Conf.*, 2017, pp. 4955–4961.

[7] R. Zhao, M. Li, Q. Niu, and Y. H. Chen, "Udwadia-Kalaba constraint-based tracking control for artificial swarm mechanical systems: Dynamic approach," *Nonlinear Dyn.*, vol. 100, no. 3, pp. 2381–2399, 2020.

[8] C.-L. Hwang and H.-H. Huang, "Experimental validation of a car-like automated guided vehicle with trajectory tracking, obstacle avoidance, and target approach," in *Proc. 43rd Annu. Conf. IEEE Ind. Electron. Soc. (IECON)*, 2017, pp. 2858–2863.

[9] C.-L. Hwang, H.-M. Wu, and J.-Y. Lai, "On-line obstacle detection, avoidance, and mapping of an outdoor quadrotor using EKF-based fuzzy tracking incremental control," *IEEE Access*, vol. 7, pp. 160203–160216, 2019.

[10] R. Aggarwal and G. Leitmann, "Avoidance control," *J. Dyn. Syst. Meas. Control*, vol. 94, no. 2, pp. 152–154, 1972.

[11] G. Leitmann and J. Skowronski, "Avoidance control," *J. Optim. Theory Appl.*, vol. 23, no. 4, pp. 581–591, 1977.

[12] M. Corless, G. Leitmann, and J. M. Skowronski, "Adaptive control for avoidance or evasion in an uncertain environment," *Comput. Math. Appl.*, vol. 13, nos. 1–3, pp. 1–11. 1987.

[13] M. Corless and G. Leitmann, "Adaptive controllers for avoidance or evasion in an uncertain environment: Some examples," *Comput. Math. Appl.*, vol. 18, nos. 1–13, pp. 161–170, 1989.

[14] L. A. Petrosjan, *Differential Games of Pursuit* (Series on Optimization), vol. 2. Singapore: World Sci., 1993.

[15] D. M. Stipanovic, P. F. Hokayem, M. W. Spong, and D. D. Šiljak, "Cooperative avoidance control for multiagent systems," *J. Dyn. Syst. Meas. Control*, vol. 129, no. 5, pp. 699–707, 2007.

[16] X. Wang, Q. Sun, and Y. H. Chen, "Adaptive robust control for triple evasion-tracing-arrival performance of uncertain mechanical systems," *J. Syst. Control Eng.*, vol. 231, no. 8, pp. 652–668, 2017.

[17] Q. Sun, X. Wang, and Y.-H. Chen, "Adaptive robust control for dual avoidance-arrival performance for uncertain mechanical systems," *Nonlinear Dyn.*, vol. 94, no. 2, pp. 759–774, 2018.

[18] V.-P. Vu and W.-J. Wang, "Polynomial controller synthesis for uncertain large-scale polynomial TS fuzzy systems," *IEEE Trans. Cybern.*, vol. 51, no. 4, pp. 1929–1942, Apr. 2021, doi: 10.1109/TCYB.2019.2895233.

[19] V.-P. Vu and W.-J. Wang, "Decentralized observer-based controller synthesis for a large-scale polynomial TS fuzzy system with nonlinear interconnection terms," *IEEE Trans. Cybern.*, vol. 51, no. 6, pp. 3312–3324, Jun. 2021, doi: 10.1109/TCYB.2019.2948647.

[20] C. Li, Y. H. Chen, H. Sun, and H. Zhao, "Optimal design of high-order control for fuzzy dynamical systems based on the cooperative game theory," *IEEE Trans. Cybern.*, vol. 52, no. 1, pp. 423–432, Jan. 2022, doi: 10.1109/TCYB.2020.2982119.

[21] Q. Sun, G. Yang, X. Wang, and Y. H. Chen, "Regulating constraint-following bound for fuzzy mechanical systems: indirect robust control and fuzzy optimal design," *IEEE Trans. Cybern.*, early access, Dec. 29, 2020, doi: 10.1109/TCYB.2020.3040680.

[22] Q. Sun, G. Yang, X. Wang, and Y.-W. Chen, "Designing robust control for mechanical systems: constraint following and multivariable optimization," *IEEE Trans. Ind. Informat.*, vol. 16, no. 8, pp. 5267–5275, Aug. 2020.

[23] J. Xu, Y. Du, H. Fang, H. Guo, and Y.-H. Chen, "A robust observer and nonorthogonal PLL-based sensorless control for fault-tolerant permanent magnet motor with guaranteed postfault performance," *IEEE Trans. Ind. Electron.*, vol. 67, no. 7, pp. 5959–5970, Jul. 2020.

[24] H. Yin, Y.-H. Chen, and D. Yu, "Stackelberg-theoretic approach for performance improvement in fuzzy systems," *IEEE Trans. Cybern.*, vol. 50, no. 5, pp. 2223–2236, May 2020.

[25] H. Sun, L. Yang, Y. H. Chen, and H. Zhao, "Constraint-based control design for uncertain underactuated mechanical system: leakage-type adaptation mechanism," *IEEE Trans. Syst., Man, Cybern., Syst.*, vol. 51, no. 12, pp. 7663–7674, Dec. 2021, doi: 10.1109/TSMC.2020.2979900.

[26] H. Wang, W. Bai, and P. X. Liu, "Finite-time adaptive fault-tolerant control for nonlinear systems with multiple faults," *IEEE/CAA J. Automatica Sinica*, vol. 6, no. 6, pp. 1417–1427, Nov. 2019.

[27] Y. H. Chen, "Approximate constraint-following of mechanical systems under uncertainty," *Nonlinear Dyn. Syst. Theory*, vol. 8, no. 4, pp. 329–337, 2008.

[28] Y. H. Chen, "Artificial swarm system: Boundedness, convergence, and control," *J. Aerosp. Eng.*, vol. 21, no. 4, pp. 288–293, 2008.

[29] Y. H. Chen, "Adaptive robust control of artificial swarm systems," *Appl. Math. Comput.*, vol. 217, no. 3, pp. 980–987, 2010.

[30] Y. Li, Y. Liu, and S. Tong, "Observer-based neuro-adaptive optimized control of strict-feedback nonlinear systems with state constraints," *IEEE Trans. Neural Netw. Learn. Syst.*, early access, Jan. 26, 2021, doi: 10.1109/TNNLS.2021.3051030.

[31] F. E. Udwadia and R. E. Kalaba, *Analytical Dynamics: A New Approach*, Cambridge, U.K.: Cambridge Univ. Press, 1996.

[32] S. E. Li, Y. Zheng, K. Li, and J. Wang, "An overview of vehicular platoon control under the four-component framework," in *Proc. IEEE Intell. Veh. Symp. (IV)*, 2015, pp. 286–291.

[33] Y. H. Chen and G. Leitmann, "Robustness of uncertain systems in the absence of matching assumptions," *Int. J. Control*, vol. 45, no. 5, pp. 1527–1542, 1987.

Qinqin Sun received the Ph.D. degree in mechanical engineering from the Nanjing University of Science and Technology, Nanjing, China, in 2021.

She worked with the Department of Mechanical Engineering, Georgia Institute of Technology, Atlanta, GA, USA, as a Research Assistant from 2014 to 2016 and visited the Department of Mechanical Engineering, University of California at Berkeley, Berkeley, CA, USA, as a visiting Ph.D. student from 2020 to 2021. She is currently an Associate Research Fellow of Aerospace Propulsion Theory and Engineering with the School of Energy and Power Engineering, Nanjing University of Aeronautics and Astronautics, Nanjing, China. Her research interests include complex system dynamics and control, fuzzy optimal design, and game theory.

Xiuye Wang received the Ph.D. degree in mechanical design and theory from the Hefei University of Technology, Hefei, China, in 2016.

He visited the Department of Mechanical Engineering, Georgia Institute of Technology, Atlanta, GA, USA, as a visiting Ph.D. student from 2014 to 2016. He is currently an Assistant Professor of Mechanical Engineering with the School of Mechanical Engineering, Nanjing University of Science and Technology, Nanjing, China. His research interests include multibody system dynamics, robust control of mechanical system, fuzzy dynamical systems, and optimal design.

Guolai Yang received the Ph.D. degree in automatic weapons and ammunition engineering from the Nanjing University of Science and Technology, Nanjing, China, in 1999.

He visited the Department of Mechanical Engineering, Texas Tech University, Lubbock, TX, USA, as a Visiting Professor in 2010. He is currently a Professor of Mechanical Engineering with the School of Mechanical Engineering and serves as the Dean of the School of International Education, Nanjing University of Science and Technology. His research interests include theory and experimental method of time-varying mechanics, mechanical system dynamics, virtual design, and simulation technique.

Ye-Hwa Chen received the Ph.D. degree in control science and engineering from the University of California at Berkeley, Berkeley, CA, USA, in 1985.

He is currently a Professor of Mechanical Engineering with the George W. Woodruff School of Mechanical Engineering, Georgia Institute of Technology, Atlanta, GA, USA, and also with the Key Laboratory of Road Construction Technology and Equipment of MOE, Chang'an University, Xi'an, Shanxi, China. His research interests include complex system dynamics, fuzzy dynamical systems, fuzzy reasoning, and modeling and control of mechanical systems.

Prof. Chen received the IEEE TRANSACTIONS ON FUZZY SYSTEMS Outstanding Paper Award from the IEEE Neural Networks Council in 2001. He was serving as a regional editor and/or an associate editor for six journals.

Fai Ma received the Ph.D. degree in applied mathematics from the California Institute of Technology, Pasadena, CA, USA, in 1981.

He was formerly a Research Engineer with the IBM Thomas J. Watson Research Center, Ossining, NY, USA, and Standard Oil Company, New York, NY, USA. He is currently a Professor of Applied Mechanics with the Department of Mechanical Engineering, University of California at Berkeley, Berkeley, CA, USA. He is the author or coauthor of more than 190 technical publications. His research interests include vibration, nonlinear damping, and system uncertainties.

Prof. Ma is a Fellow of the American Society of Mechanical Engineers.